Available online at www.sciencedirect.com
ScienceDirect
Comput. Methods Appl. Mech. Engrg. xxx (2007) xxx–xxx
Computer methods in applied mechanics and engineering
www.elsevier.com/locate/cma

A sampling-based computational strategy for the representation of epistemic uncertainty in model predictions with evidence theory

J.C. Helton [a,*], J.D. Johnson [b], W.L. Oberkampf [c], C.B. Storlie [d]

[a] Department of Mathematics and Statistics, Arizona State University, Tempe, AZ 85287-1804, USA
[b] ProStat, Mesa, AZ 85204-5326, USA
[c] Sandia National Laboratories, Albuquerque, NM 87185-0828, USA
[d] Department of Statistics, North Carolina State University, Raleigh, NC 27695, USA

Received 1 November 2005; accepted 30 October 2006

Abstract

Evidence theory provides an alternative to probability theory for the representation of epistemic uncertainty in model predictions that derives from epistemic uncertainty in model inputs, where the descriptor epistemic is used to indicate uncertainty that derives from a lack of knowledge with respect to the appropriate values to use for various inputs to the model. The potential benefit, and hence appeal, of evidence theory is that it allows a less restrictive specification of uncertainty than is possible within the axiomatic structure on which probability theory is based. Unfortunately, the propagation of an evidence theory representation for uncertainty through a model is more computationally demanding than the propagation of a probabilistic representation for uncertainty, with this difficulty constituting a serious obstacle to the use of evidence theory in the representation of uncertainty in predictions obtained from computationally intensive models. This presentation describes and illustrates a sampling-based computational strategy for the representation of epistemic uncertainty in model predictions with evidence theory. Preliminary trials indicate that the presented strategy can be used to propagate uncertainty representations based on evidence theory in analysis situations where naïve sampling-based (i.e., unsophisticated Monte Carlo) procedures are impracticable due to computational cost.
© 2007 Published by Elsevier B.V.

Keywords: Dempster–Shafer theory; Epistemic uncertainty; Evidence theory; Monte Carlo; Numerical uncertainty propagation; Sensitivity analysis; Uncertainty analysis

1. Introduction

An appropriate representation of the uncertainty in analysis outcomes is an essential part of any complete analysis [1,2]. Specifically, an analysis that is intended to provide insights into the behavior of a system or the basis for decisions must provide an assessment of the uncertainty associated with its outcomes. Without such an assessment, neither insights drawn from the analysis nor decisions based on it are adequately informed and supported.

Analyses of the behavior of complex systems typically involve two types of uncertainty: aleatory and epistemic [3,4]. Aleatory uncertainty arises from what is considered to be an inherent randomness in the behavior of the system under study. For example, in a risk assessment for a chemical plant, the weather conditions at the time of an accident are usually considered to be an aleatory uncertainty. Epistemic uncertainty arises from a lack of knowledge about a quantity that is assumed to have a fixed value in the context of a particular analysis. For example, the pressure at which a specific reactor containment will fail is presumably fixed but certainly unknown and is thus an epistemic uncer-

* Corresponding author. Present address: Department 6849, MS 0779, Sandia National Laboratories, Albuquerque, NM 87185-0828, USA. Tel.: +1 505 284 4808; fax: +1 505 844 2348.
E-mail address: jchelto@sandia.gov (J.C. Helton).

0045-7825/$ - see front matter © 2007 Published by Elsevier B.V.
doi:10.1016/j.cma.2006.10.049

UNCORRECTED PROOF

tainty. As an example, probabilistic risk assessments for nuclear power plants are typically designed to maintain a separation between aleatory uncertainty and epistemic uncertainty [5].

Probability has traditionally been employed as the mathematical structure used to represent both aleatory uncertainty and epistemic uncertainty [6]. With this usage, an analysis maintaining a separation of aleatory uncertainty and epistemic uncertainty involves two probability spaces: a probability space characterizing aleatory uncertainty and a probability space characterizing epistemic uncertainty. However, many individuals have reservations about the use of probability to represent epistemic uncertainty when there is limited information available on which to base a fully structured development of probability. In particular, the concern is that the definition of a full probabilistic description of uncertainty entails an implication of a higher resolution of knowledge than is really present.

Evidence theory provides an alternative to probability theory for the representation of epistemic uncertainty in model predictions that derives from epistemic uncertainty in model inputs [7]. The potential benefit, and hence appeal, of evidence theory is that it allows a less restrictive specification of uncertainty than is possible within the axiomatic structure on which probability theory is based. Unfortunately, the propagation of an evidence theory representation for uncertainty through a model is more computationally demanding than the propagation of a probabilistic representation for uncertainty, with this difficulty constituting a serious obstacle to the use of evidence theory in the representation of uncertainty in predictions obtained from computationally intensive models. This presentation describes and illustrates a sampling-based computational strategy for the representation of epistemic uncertainty in model predictions with evidence theory. Preliminary trials indicate that the presented strategy can be used to propagate uncertainty representations based on evidence theory in analysis situations where naïve sampling-based (i.e., unsophisticated Monte Carlo) procedures are impracticable due to computational cost.

2. Evidence theory

An analysis can be conceptually represented in the functional form $\mathbf{y} = f(\mathbf{x})$, where $\mathbf{x} = [x_1, x_2, \ldots, x_{nX}]$ is a vector of analysis inputs, $\mathbf{y} = [y_1, y_2, \ldots, y_{nY}]$ is a vector of analysis results, and f is a function that maps $\mathbf{x}$ into $\mathbf{y}$. In practice, f can be quite complex and, as examples, could involve the solution of a system of nonlinear partial differential equations or the operation of a sequence of linked models. Further, the dimensionality of $\mathbf{x}$ and $\mathbf{y}$ is often high (e.g., on the order of 100 s).

Probability theory provides the mathematical structure that has been traditionally used to characterize the epistemic uncertainty in results obtained in analyses of the form just indicated. With this approach, the uncertainty in the elements of $\mathbf{x}$ is represented by a sequence of distributions $D_1, D_2, \ldots, D_{nX}$, where D_j is a distribution that characterizes the uncertainty associated with the element x_j of $\mathbf{x}$. Various correlations and other restrictions involving the elements of $\mathbf{x}$ may also be specified. Typically, the distributions $D_1, D_2, \ldots, D_{nX}$ are developed through some form of expert review process [8]. Conceptually, these distributions give rise to a probability space $(\mathcal{X}_P, \mathbb{X}_P, m_{PX})$ that characterizes the uncertainty in $\mathbf{x}$, where (i) $\mathcal{X}_P$ is the set (i.e., sample space) of possible values for $\mathbf{x}$, (ii) $\mathbb{X}_P$ is an appropriately defined set of subsets of $\mathcal{X}_P$ (i.e., a σ-algebra), and (iii) m_{PX} is a function (i.e., a probability measure) that defines the probability of individual elements of $\mathbb{X}_P$. For notational convenience, the uncertainty in $\mathbf{x}$ characterized by the distributions $D_1, D_2, \ldots, D_{nX}$ and the associated probability space $(\mathcal{X}_P, \mathbb{X}_P, m_{PX})$ can be represented by a density function $d_X(\mathbf{x})$ defined on $\mathcal{X}_P$.

In turn, the uncertainty in $\mathbf{x}$ gives rise to uncertainty in the elements of $\mathbf{y}$. For notational convenience in the following discussion, $\mathbf{y}$ is assumed to consist of a single real-valued component y; specifically, $y = f(\mathbf{x})$ is under consideration. This eliminates the need to use subscripting to identify individual elements of $\mathbf{y}$ but does not otherwise alter the discussion. In concept, the uncertainty in y is characterized by a probability space $(\mathcal{Y}_P, \mathbb{Y}_P, m_{PY})$ and an associated density function $d_Y(y)$ defined on $\mathcal{Y}_P$ that derive from the properties of the probability space $(\mathcal{X}_P, \mathbb{X}_P, m_{PX})$ and the function f.

In practice, the uncertainty in y is summarized by an estimated cumulative or complementary cumulative distribution function (i.e., a CDF or CCDF). Specifically, the CDF and CCDF for y are defined by the probabilities

$$\mathrm{prob}(\tilde{y} \leqslant y) = \int_{\mathcal{X}_P} \underline{\delta}[f(\mathbf{x})|y] d_X(\mathbf{x}) \mathrm{d}X \cong \sum_{i=1}^{nS} \underline{\delta}[f(\mathbf{x}_i)|y]/nS \tag{2.1}$$

and

$$\mathrm{prob}(\tilde{y} > y) = \int_{\mathcal{X}_P} \bar{\delta}[f(\mathbf{x})|y] d_X(\mathbf{x}) \mathrm{d}X \cong \sum_{i=1}^{nS} \bar{\delta}[f(\mathbf{x}_i)|y]/nS, \tag{2.2}$$

respectively, where

$$\underline{\delta}[f(\mathbf{x})|y] = \begin{cases} 1 & \text{if } f(\mathbf{x}) \leqslant y, \\ 0 & \text{if } f(\mathbf{x}) > y, \end{cases} \quad \bar{\delta}[f(\mathbf{x})|y] = 1 - \underline{\delta}[f(\mathbf{x})|y] = \begin{cases} 0 & \text{if} f(\mathbf{x}) \leqslant y, \\ 1 & \text{if} f(\mathbf{x}) > y \end{cases}$$

and $\mathbf{x}_i = [x_{i1}, x_{i2}, \ldots, x_{i,nX}]$, $i = 1, 2, \ldots, nS$ is a random or Latin hypercube sample [9,10] of size nS from $\mathcal{X}_P$ generated in consistency with the previously indicated distributions $D_1, D_2, \ldots, D_{nX}$. Latin hypercube sampling is often used in analyses of this type because of its efficient stratification properties.

UNCORRECTED PROOF

Please cite this article in press as: J.C. Helton et al., A sampling-based computational strategy for the representation ..., Comput. Methods Appl. Mech. Engrg. (2007), doi:10.1016/j.cma.2006.10.049

Given that the probabilities in Eqs. (2.1) and (2.2) can be determined, the CDF and CCDF for y are formally defined by the sets

$$\mathcal{CDF} = \{[y, \mathrm{prob}_Y(\tilde{y} \leqslant y)] : y \in \mathcal{Y}_P\} \cong \left\{ \left[y, \sum_{i=1}^{nS} \bar{\delta}[f(\mathbf{x}_i)|y] \Big/ nS : y \in \mathcal{Y}_P \right\} \tag{2.3}$$

and

$$\mathcal{CCDF} = \{[y, \mathrm{prob}_Y(\tilde{y} > y)] : y \in \mathcal{Y}_P\} \cong \left\{ \left[y, \sum_{i=1}^{nS} \underline{\delta}[f(\mathbf{x}_i)|y] \Big/ nS : y \in Y_{\mathcal{P}} \right\}, \tag{2.4}$$

respectively.

The uncertainty in y can also be represented with the expected value $E(y)$ and variance $V(y)$ of y given by

$$E(y) = \int_{\mathcal{X}_P} f(\mathbf{x}) d_X(\mathbf{x}) \mathrm{d}X \cong \sum_{i=1}^{nS} f(\mathbf{x}_i)/nS \tag{2.5}$$

and

$$V(y) = \int_{X_P} [f(\mathbf{x}) - E(y)]^2 d_X(\mathbf{x}) \mathrm{d}X \cong \sum_{i=1}^{nS} \left[f(\mathbf{x}_i) - \sum_{i=1}^{nS} f(\mathbf{x}_i) \Big/ nS \right]^2 \Big/ (nS - 1), \tag{2.6}$$

respectively, where $\mathbf{x}_i$, $i = 1, 2, \ldots, nS$, is the sample indicated in conjunction with Eqs. (2.1) and (2.2). However, a large amount of information is lost when only $E(y)$ and $V(y)$ are used to represent the uncertainty in y as the information given by nS results has been coalesced into only two numbers. As a result, CDFs and CCDFs provide more informative representations of uncertainty than means and variances.

The results used in the estimation of the CDF and CCDF in Eqs. (2.3) and (2.4) constitute a mapping

$$[\mathbf{x}_i, f(\mathbf{x}_i)] = [x_{i1}, x_{i2}, \ldots, x_{i,nX}, y_i], \quad i = 1, 2, \ldots, nS, \tag{2.7}$$

between analysis inputs and analysis results, where $y_i = f(\mathbf{x}_i)$. Once generated, this mapping can be investigated with a variety of sensitivity analysis procedures [8]. Such sensitivity analyses constitute an important part of analyses employing a sampling-based propagation of uncertainty.

Analyses based on probabilistic characterization of epistemic uncertainty are very popular and have been widely used [8,10]. However, such analyses are open to the criticism that there may not be enough information available to justify the definition of the distributions $D_1, D_2, \ldots, D_{nX}$. In particular, defining a probability distribution for an element x_j of $\mathbf{x}$ imposes a large amount of structure on the characterization of the uncertainty with respect to what the appropriate value for x_j is. When there is little information about the value of a variable, this imposed structure may not be appropriate. For example, there is a large difference in concept and implication between saying that all that is known about a quantity is that its value is located somewhere in an interval $[a, b]$ and saying that a uniform distribution on $[a, b]$ characterizes degrees of belief with respect to where the value of this quantity is located in the interval $[a, b]$.

Several alternatives to probability theory for the representation of uncertainty have been proposed, including interval analysis, possibility theory, fuzzy set theory, and evidence theory [11–18]. The introduction of these alternatives to probability theory for the representation of epistemic uncertainty has been accompanied by a lively debate with respect to their appropriateness and usefulness, with some analysts maintaining that probability theory is the only appropriate mathematical structure for the representation of uncertainty and other analysts maintaining that these alternative uncertainty representations are essential to an appropriate representation of uncertainty in the presence of limited information [7]. While not rejecting all use of probability theory to represent epistemic uncertainty, the authors of this paper feel that the indicated alternative mathematical structures for the representation of uncertainty do have useful roles to play when uncertainty must be characterized, and decisions made, on the basis of limited information.

The focus of this paper is on evidence theory, which provides a less structured representation of uncertainty than probability theory and yet is still closely related to probability theory. Indeed, an uncertainty representation with evidence theory approaches an uncertainty representation with probability theory as the amount of information and/or insight available for use in the characterization of uncertainty increases. The authors find this connection to be very appealing. Evidence theory is also sometimes referred to as Dempster–Shafer theory in recognition of the early development work of these two individuals [19–22].

Just as a probability space involving a quantity $\mathbf{x}$ is the basic mathematical structure in probability theory, an evidence space involving a quantity $\mathbf{x}$ is the basic mathematical structure in evidence theory. Similarly to a probability space for $\mathbf{x}$, an evidence space for $\mathbf{x}$ is a triple of the form $(X_E, \mathbb{X}_E, m_{EX})$, where (i) $\mathcal{X}_E$ is the set (i.e., sample space or universal set) of possible values of $\mathbf{x}$, (ii) $\mathbb{X}_E$ is a set of subsets of $\mathcal{X}_E$, and (iii) m_{EX} is a function satisfying the conditions

$$m_{EX}(\mathcal{U}) > 0 \quad \text{if } \mathcal{U} \subset \mathcal{X}_E \text{ and } \mathcal{U} \in \mathbb{X}_E, \tag{2.8}$$

$$m_{EX}(\mathcal{U}) = 0 \quad \text{if } \mathcal{U} \subset \mathcal{X}_E \text{ and } \mathcal{U} \notin \mathbb{X}_E \tag{2.9}$$

and

$$\sum_{\mathcal{U} \in \mathbb{X}_E} m_{EX}(\mathcal{U}) = 1. \tag{2.10}$$

The numeric value $m_{EX}(\mathcal{U})$ is referred to as the basic probability assignment (BPA) for a subset $\mathcal{U}$ of $\mathcal{X}_E$, and the elements of $\mathbb{X}_E$ (i.e., the subsets of $\mathcal{X}_E$ with nonzero BPAs) are referred to as the focal elements of the evidence space.

The sets $\mathcal{X}_P$ and $\mathcal{X}_E$ associated with a probability space $(\mathcal{X}_P, \mathbb{X}_P, m_{PX})$ and an evidence space $(\mathcal{X}_E, \mathbb{X}_E, m_{EX})$ for a

UNCORRECTED PROOF

Please cite this article in press as: J.C. Helton et al., A sampling-based computational strategy for the representation ..., Comput. Methods Appl. Mech. Engrg. (2007), doi:10.1016/j.cma.2006.10.049

quantity $\mathbf{x}$ are conceptually the same as both $\mathcal{X}_P$ and $\mathcal{X}_E$ simply contain all possible values for $\mathbf{x}$. However, the sets $\mathbb{X}_P$ and $\mathbb{X}_E$ and the functions m_{PX} and m_{EX} are conceptually different. Collectively, the sets in $\mathbb{X}_P$ constitute a σ-algebra; specifically, (i) if $\mathcal{U} \in \mathbb{X}_P$, then $\mathcal{U}^c \in \mathbb{X}_P$, where $\mathcal{U}^c$ is the complement of $\mathcal{U}$, and (ii) if $\mathcal{U}_1, \mathcal{U}_2, \ldots$, is a sequence of elements of $\mathbb{X}_P$, then $\cup_i \mathcal{U}_i \in \mathbb{X}_P$ and $\cap_i \mathcal{U}_i \in \mathbb{X}_P$. In contrast, there is no specified structure associated with $\mathbb{X}_E$ as the membership of a subset $\mathcal{U}$ of $\mathcal{X}_E$ in $\mathbb{X}_E$ is defined solely by the property $m_{EX}(\mathcal{U}) > 0$. Further, $\mathbb{X}_P$ has an uncountably infinite number of elements in most developments of probability while $\mathbb{X}_E$ can never have more than a countably infinite number of elements and usually has a finite number of elements.

The function m_{PX} defines the probability associated with elements of $\mathbb{X}_P$ and is referred to as a probability measure. Specifically, (i) if $\mathcal{U} \in \mathbb{X}_P$, then $0 \leqslant m_{PX}(\mathcal{U}) \leqslant 1$, (ii) $m_{PX}(\mathcal{X}_P) = 1$, and (iii) if $\mathcal{U}_1, \mathcal{U}_2, \ldots$ is a sequence of disjoint sets from $\mathbb{X}_P$, then $m_{PX}(\cup_i \mathcal{U}_i) = \sum_i m_{PX}(\mathcal{U}_i)$. A fundamental property of probability that results from the preceding is

$$m_{PX}(\mathcal{U}) + m_{PX}(\mathcal{U}^c) = 1 \tag{2.11}$$

for $\mathcal{U} \in \mathbb{X}_P$. In contrast, less structure is imposed on m_{EX} as only the relationships in Eqs. (2.8)–(2.10) are required to hold. Conceptually, $m_{EX}(\mathcal{U})$ can be interpreted as the amount of information (i.e., level of credibility or probability) that can be assigned to $\mathcal{U}$ but can in no known way be assigned to any subset of $\mathcal{U}$.

Probability theory has only one measure of uncertainty: probability, which is defined by the function m_{XP}. In contrast, evidence theory has two measures of uncertainty: belief and plausibility, which are derived from the function m_{EX}. Specifically, the belief $\mathrm{Bel}_X(\mathcal{U})$ and plausibility $\mathrm{Pl}_X(\mathcal{U})$ of a subset $\mathcal{U}$ of $\mathcal{X}_E$ are defined by

$$\mathrm{Bel}_X(\mathcal{U}) = \sum_{\mathcal{V} \subset \mathcal{U}} m_{EX}(\mathcal{V}) \text{ and } \mathrm{Pl}_X(\mathcal{U}) = \sum_{\mathcal{V} \cap \mathcal{U} \neq \emptyset} m_{EX}(\mathcal{V}). \tag{2.12}$$

Intuitively, $\mathrm{Bel}_X(\mathcal{U})$ provides a measure of the amount of information that supports $\mathcal{U}$ being true (e.g., that $\mathcal{U}$ contains the true value for the epistemically uncertain quantity $\mathbf{x}$), and $\mathrm{Pl}_X(\mathcal{U})$ provides a measure of the absence of information that supports $\mathcal{U}$ being false (e.g., that $\mathcal{U}$ does not contain the true value for the epistemically uncertain quantity $\mathbf{x}$). Thus, for example, $\mathrm{Bel}_X(\mathcal{U}) = 0$ indicates that none of the available information unambiguously supports $\mathcal{U}$ being true (i.e., no focal element of the evidence space is a subset of $\mathcal{U}$), and $\mathrm{Pl}_X(\mathcal{U}) = 1$ indicates that none of the available information unambiguously supports $\mathcal{U}$ being false (i.e., every focal element of the evidence space intersects $\mathcal{U}$).

The preceding definitions and interpretations for belief and plausibility arise from viewing the BPA associated with a focal element of an evidence space as providing a measure of the amount of information that can be assigned to a set but cannot be specifically assigned to any subset of that set. Thus, as a result of the subset requirement in the definition of belief in Eq. (2.12), belief provides a measure of the amount of information that has to be assigned to a set. In contrast, as a result of the intersection requirement in the definition of plausibility in Eq. (2.12), plausibility provides a measure of the total amount of information that could possibly be assigned to a set or, equivalently, a measure of the absence of information that cannot be assigned to the set. The names belief and plausibility for the mathematical entities defined in Eq. (2.12) are intuitively suggestive of the ideas indicated in the preceding discussion, with "belief" suggesting how strongly it is felt that something is true and "plausibility" suggesting how strongly it is felt that something might be true.

The following relationships hold for belief and plausibility and a subset $\mathcal{U}$ of $\mathcal{X}_E$:

$$\begin{aligned} &\mathrm{Bel}_X(\mathcal{U}) + \mathrm{Bel}_X(\mathcal{U}^c) \leqslant 1, \\ &\mathrm{Pl}_X(\mathcal{U}) + \mathrm{Pl}_X(\mathcal{U}^c) \geqslant 1, \\ &\mathrm{Pl}_X(\mathcal{U}) + \mathrm{Bel}_X(\mathcal{U}^c) = 1. \end{aligned} \tag{2.13}$$

Thus, unlike the probabilistic relationship in Eq. (2.11), the belief assigned to a set does not uniquely determine the belief assigned to its complement, and similarly, the plausibility assigned to a set does not uniquely determine the plausibility assigned to its complement. Further, (i) both a set and its complement can have beliefs that are equal to or close to zero, (ii) both a set and its complement can have plausibilities that are equal to or close to one, and (iii) a set can have plausibility close to one only if the belief in the complement of that set is close to zero.

As previously indicated, the use of probability theory to characterize the epistemic uncertainty associated with the vector $\mathbf{x}$ is accomplished by assigning a probability distribution D_j to each element x_j of $\mathbf{x}$. In concept, this corresponds to developing a probability space $(\mathcal{X}_{Pj}, \mathbb{X}_{Pj}, m_{Pj})$ for each x_j and then developing the probability space $(\mathcal{X}_P, \mathbb{X}_P, m_{PX})$ characterizing the uncertainty in $\mathbf{x}$ from these probability spaces. Of course, this level of formality is never used in practice as defining the D_j by specifying CDFs (or density functions, which give rise to CDFs) is all that is needed for the description and computational implementation of an analysis. However, the concept of probability spaces for the individual elements of $\mathbf{x}$ is introduced to make a conceptual and notational connection with what is done when evidence theory is used to characterize the epistemic uncertainty associated with the elements of $\mathbf{x}$.

When evidence theory is used to represent the epistemic uncertainty associated with the elements of $\mathbf{x}$, an evidence space $(\mathcal{X}_{Ej}, \mathbb{X}_{Ej}, m_{Ej})$ is defined to characterize the uncertainty associated with each element x_j of $\mathbf{x}$, where (i) $\mathcal{X}_{Ej}$ is the set of possible values for x_j, (ii) $\mathbb{X}_{Ej} = \{\mathcal{U}_{j1}, \mathcal{U}_{j2}, \ldots, \mathcal{U}_{j,n(j)}\}$ is the set of focal elements for x_j, and (iii) the function m_{Ej} defines the BPA for each subset of X_{Ej}. In turn, the evidence spaces $(\mathcal{X}_{Ej}, \mathbb{X}_{Ej}, m_{Ej})$ for the individual

UNCORRECTED PROOF

Please cite this article in press as: J.C. Helton et al., A sampling-based computational strategy for the representation ..., Comput. Methods Appl. Mech. Engrg. (2007), doi:10.1016/j.cma.2006.10.049

elements of $\mathbf{x}$ give rise to the evidence space $(\mathcal{X}_E, \mathbb{X}_E, m_{EX})$ for $\mathbf{x}$. Specifically,

$$\mathcal{X}_E = X_{E1} \times \mathcal{X}_{E2} \times \cdots \times \mathcal{X}_{E,nX}, \tag{2.14}$$

$$\mathbb{X}_E = \{\mathcal{U} : \mathcal{U} = \mathcal{U}_{1r} \times \mathcal{U}_{2s} \times \cdots \times \mathcal{U}_{nX,t}, 1 \leqslant r \leqslant n(1), 1 \leqslant s \leqslant n(2), \ldots, 1 \leqslant t \leqslant n(nX)\} \tag{2.15}$$

and

$$m_{XE}(\mathcal{U}) = \begin{cases} m_{E1}(\mathcal{U}_{1r}) m_{E2}(\mathcal{U}_{2s}), \ldots, m_{E,nX}(\mathcal{U}_{nX,t}) \\ \quad \text{if } \mathcal{U} = \mathcal{U}_{1r} \times \mathcal{U}_{2s} \times \cdots \times \mathcal{U}_{nX,t} \in \mathbb{X}_E, \\ 0 \quad \text{otherwise.} \end{cases} \tag{2.16}$$

The number of sets (i.e., focal elements) in $\mathbb{X}_E$ is given by $n = \prod_{j=1}^{nX} n(j)$, which can become quite large as nX and the individual $n(j)$s increase in size. The preceding definition for $(\mathcal{X}_E, \mathbb{X}_E, m_{EX})$ is based on the assumption that the x_js are independent. The development of an evidence space for $\mathbf{x}$ is considerably more complicated if the x_js are not independent and is not considered here [23].

Characterization of the epistemic uncertainty in $\mathbf{x}$ with probability (i.e., with the uncertainty in $\mathbf{x}$ characterized by a probability space $(\mathcal{X}_P, \mathbb{X}_P, m_{PX})$) results in the uncertainty in $y = f(\mathbf{x})$ also bring characterized by a probability space $(\mathcal{Y}_P, \mathbb{Y}_P, m_{PY})$ that derives from the properties of $(\mathcal{X}_P, \mathbb{X}_P, m_{PX})$ and the function f. Similarly, the characterization of the epistemic uncertainty in $\mathbf{x}$ with an evidence theory representation (i.e., with the uncertainty in $\mathbf{x}$ characterized by an evidence space $(\mathcal{X}_E, \mathbb{X}_E, m_{EX})$) results in the uncertainty in $y = f(\mathbf{x})$ also being characterized by an evidence space $(\mathcal{Y}_E, \mathbb{Y}_E, m_{EY})$ that derives from the properties of $(\mathcal{X}_E, \mathbb{X}_E, m_{EX})$ and the function f.

In practice, the evidence space $(\mathcal{Y}_E, \mathbb{Y}_E, m_{EY})$ is unlikely to be constructed in a real analysis. If f is expensive to evaluate, the computational cost of generating a reasonable approximation to $(\mathcal{Y}_E, \mathbb{Y}_E, m_{EY})$ is likely to be prohibitive. Instead, the uncertainty associated with y is likely to be summarized with a cumulative belief function and a cumulative plausibility function (i.e., a CBF and a CPF) or a complementary cumulative belief function and a complementary cumulative plausibility function (i.e., a CCBF and a CCPF). Similarly to the defining probabilities for a CDF and CCDF in Eqs. (2.1) and (2.2), the defining beliefs and plausibilities for a CBF, CCBF, CPF and CCPF are given by

$$\begin{aligned} \mathrm{Bel}_Y(\tilde{y} \leqslant y) &= \sum_{\mathcal{U} \subset \mathcal{U}_y} m_{EY}(\mathcal{U}), \\ \mathrm{Bel}_Y(\tilde{y} > y) &= \sum_{\mathcal{U} \subset \mathcal{U}_y^c} m_{EY}(\mathcal{U}), \end{aligned} \tag{2.17}$$

$$\begin{aligned} \mathrm{Pl}_Y(\tilde{y} \leqslant y) &= \sum_{\mathcal{U} \cap \mathcal{U}_y \neq \emptyset} m_{EY}(\mathcal{U}) \quad \text{and} \\ \mathrm{Pl}_Y(\tilde{y} > y) &= \sum_{\mathcal{U} \cap \mathcal{U}_y^c \neq \emptyset} m_{EY}(\mathcal{U}), \end{aligned} \tag{2.18}$$

respectively, where $\mathcal{U}_y = \{\tilde{y} : \tilde{y} \in \mathcal{Y}_E \text{ and } \tilde{y} \leqslant y\}$ is the set of all values in $\mathcal{Y}_E$ that are less than or equal to y. The CBF, CCBF, CPF and CCPF for y are then formally defined by the sets

$$\begin{aligned} \mathcal{CBF} &= \{[y, \mathrm{Bel}_Y(\tilde{y} \leqslant y)] : y \in \mathcal{Y}_E\}, \\ \mathcal{CCBF} &= \{[y, \mathrm{Bel}_Y(\tilde{y} > y)] : y \in \mathcal{Y}_E\}, \end{aligned} \tag{2.19}$$

$$\begin{aligned} \mathcal{CPF} &= \{[y, \mathrm{Pl}_Y(\tilde{y} \leqslant y)] : y \in \mathcal{Y}_E\} \quad \text{and} \\ \mathcal{CCPF} &= \{[y, \mathrm{Pl}_Y(\tilde{y} > y)] : y \in \mathcal{Y}_E\}, \end{aligned} \tag{2.20}$$

respectively. Analogous definitions for a CDF and a CCDF are given in Eqs. (2.3) and (2.4).

As formally presented in Eqs. (2.17) and (2.18), the evaluation of $\mathrm{Bel}_Y(\tilde{y} \leqslant y), \mathrm{Bel}_Y(\tilde{y} > y), \mathrm{Pl}_Y(\tilde{y} \leqslant y)$ and $\mathrm{Pl}_Y(\tilde{y} > y)$ requires knowledge of all the focal elements in $\mathbb{Y}_E$ and their associated BPAs. Such information is unlikely to be determined in a real analysis. Rather, a more likely approach is to use a sampling-based procedure to estimate $\mathrm{Bel}_Y(\tilde{y} \leqslant y), \mathrm{Bel}_Y(\tilde{y} > y), \mathrm{Pl}_Y(\tilde{y} \leqslant y)$ and $\mathrm{Pl}_Y(\tilde{y} > y)$. With this approach, the indicated beliefs and plausibilities are estimated by

$$\begin{aligned} \mathcal{CBF} &= \{[y, \mathrm{Bel}_X(f^{-1}[\mathcal{U}_y])] : y \in \mathcal{Y}_E\} \\ &= \{[y, 1 - \mathrm{Pl}_X(f^{-1}[\mathcal{U}_y^c])] : y \in \mathcal{Y}_E\} \\ &\cong \{[y_i, 1 - \mathrm{Pl}_X(\{\mathbf{x}_j : y_j > y_i\})] : i = 1, 2, \ldots, nS\}, \end{aligned} \tag{2.21}$$

$$\begin{aligned} \mathcal{CCBF} &= \{[y, \mathrm{Bel}_X(f^{-1}[\mathcal{U}_y^c])] : y \in \mathcal{Y}_E\} \\ &= \{[y, 1 - \mathrm{Pl}_X(f^{-1}[\mathcal{U}_y])] : y \in \mathcal{Y}_E\} \\ &\cong \{[y_i, 1 - \mathrm{Pl}_X(\{\mathbf{x}_j : y_j \leqslant y_i\})] : i = 1, 2, \ldots, nS\}, \end{aligned} \tag{2.22}$$

$$\begin{aligned} \mathcal{CPF} &= \{[y, \mathrm{Pl}_X(f^{-1}[\mathcal{U}_y])] : y \in \mathcal{Y}_E\} \\ &\cong \{[y_i, \mathrm{Pl}_X(\{\mathbf{x}_j : y_j \leqslant y_i\})] : i = 1, 2, \ldots, nS\}, \end{aligned} \tag{2.23}$$

and

$$\begin{aligned} \mathcal{CCPF} &= \{[y, \mathrm{Pl}_X(f^{-1}[\mathcal{U}_y^c])] : y \in \mathcal{Y}_E\} \\ &\cong \{[y_i, \mathrm{Pl}_X(\{\mathbf{x}_j : y_j > y_i\})] : i = 1, 2, \ldots, nS\}, \end{aligned} \tag{2.24}$$

where

$$[\mathbf{x}_i, \mathbf{y}_i] = [\mathbf{x}_i, f(\mathbf{x}_i)], i = 1, 2, \ldots, nS, \tag{2.25}$$

is a mapping between $\mathcal{X}_E$ and $\mathcal{Y}_E$ defined by a suitable sample from $\mathcal{X}_E$. The conversion from belief to plausibility in Eqs. (2.21) and (2.22) through the use of the equality in Eq. (2.13) is necessary because the subset relationship that defines belief cannot be determined with a finite sample when the sets $\mathcal{U}_y$ and $\mathcal{U}_y^c$ contain infinitely many elements (which is usually the case).

In concept, any sampling strategy can be used to generate the mapping in Eq. (2.25) as long as the sampled points provide adequate coverage of the focal elements in $\mathbb{X}_E$ as the sample size nS increases (e.g., provided the sampled points tend to become dense in $\mathcal{X}_E$ as nS increases) [24,25]. If the focal elements for the elements x_j of $\mathbf{x}$ are intervals of the form $I_{jk} = \{x_j : a_{jk} \leqslant x_j \leqslant b_{jk}\}$, a sampling

UNCORRECTED PROOF

distribution for each x_j for use in generating the mapping in Eq. (2.25) can be defined by the density function

$$d_j(x_j) = \sum_{k=1}^{n(j)} \delta(x_j|I_{jk}) m_{jE}(I_{jk})/(b_{jk} - a_{jk})$$

$$\text{where } \delta(x_j|I_{jk}) = \begin{cases} 1 & \text{if } x_j \in I_{jk}, \\ 0 & \text{if } x_j \notin I_{jk}. \end{cases} \tag{2.26}$$

Then, the corresponding sampling distribution for $\mathbf{x}$ is defined by the density function

$$d(\mathbf{x}) = \prod_{j=1}^{nX} d_j(x_j). \tag{2.27}$$

This distribution is appealing as it preserves some of the character and emphasis of the underlying evidence space $(\mathcal{X}_E, \mathbb{X}_E, m_{EX})$ that has been developed from the evidence spaces $(\mathcal{X}_{Ej}, \mathbb{X}_{Ej}, m_{Ej})$, $j = 1, 2, \ldots, nX$, defined for the individual components of $\mathbf{x}$.

Unfortunately, there is a dimensionality challenge in the implementation of calculations involving evidence theory representations for uncertainty. Specifically, the cardinality n of the set $\mathbb{X}_E$ defined in Eq. (2.15) increases rapidly with increasing values for the number nX of components of $\mathbf{x}$ and the number $n(j)$ of focal elements associated with each component x_j of $\mathbf{x}$. For example, $n = \prod_{j=1}^{nX} n(j) = 10^{15}$ when $nX = 15$ and $n(j) = 10$ for $j = 1, 2, \ldots, nX$. The computational challenge results because obtaining evidence theory results for y (e.g., as defined by the CBF, CCBF, CPF and CCPF in Eqs. (2.19) and (2.20)) and the associated approximations in Eqs. (2.21)–(2.24) effectively requires determining, or at least estimating, the minimum and maximum value of y for each focal element in $\mathbb{X}_E$. When n is large and/or the evaluation of $f(\mathbf{x})$ is computationally demanding, the number of evaluations of $f(\mathbf{x})$ needed to obtain the approximations of the CBF, CCBF, CPF and CCPF for y in Eqs. (2.21)–(2.24) or to directly estimate the BPAs for all focal elements associated with the evidence space $(\mathcal{Y}_E, \mathbb{Y}_E, m_{EY})$ is computationally impracticable. The purpose of this presentation is to describe and illustrate a computational strategy for the determination of the CBF, CCBF, CPF and CCPF for y that can be successfully employed when the cardinality n of $\mathbb{X}_E$ is large.

3. Computational strategy for estimating CBF, CCBF, CPF and CCPF for y

The computational strategy for estimating the CBF, CCBF, CPF and CCPF for y involves the following initial steps:

Step 1. Define a sampling distribution for $\mathbf{x}$ based on the specified evidence theory structure for the uncertain model inputs. The probability distribution defined by the density function in Eq. (2.27) is recommended for use here because of its match to the general character of the evidence space for $\mathbf{x}$.

Step 2. Generate a Latin hypercube sample [9,10] from the uncertain inputs with the sampling distribution defined in Step 1. The outcome of this step is a sample of the form indicated in conjunction with Eqs. (2.1) and (2.2). In general, analyses will contain large numbers of both uncertain input variables and uncertain predicted variables (i.e., nX and nY as indicated in the definitions of $\mathbf{x}$ and $\mathbf{y}$ in Section 2). As a result, it is difficult to develop an *a priori* sampling plan based on anticipated relationships between the elements of $\mathbf{x}$ and the elements of $\mathbf{y}$. Under these conditions, Latin hypercube sampling is a very effective sampling strategy because its dense stratification across the range of each uncertain input results in a good representation of model behavior regardless of which predicted variable is under consideration and which elements of $\mathbf{x}$ actually affect the uncertainty in this variable.

Step 3. Propagate the sample generated in Step 2 through the model to obtain values for all model results of interest. Specifically, this corresponds to generating the mapping between uncertain input variables and uncertain predicted variables indicated in Eq. (2.7), where in general y_i is a vector of dimension nY rather than a scalar.

The following additional steps are then performed individually for each model result y of interest. As previously indicated, most analyses will involve the consideration of a large number of individual results.

Step 4. Perform a sensitivity analysis to identify which of the uncertain model inputs, say $x_1, x_2, \ldots, x_r$ ordered by importance, are significant contributors to the uncertainty associated with y. This sensitivity analysis is based on an exploration of the mapping in Eq. (2.7) generated in Step 3 for the particular y under consideration. A variety of sensitivity analysis procedures are available for use in this step [8].

Step 5. Use the results of Step 3 and an appropriate regression procedure to develop a response surface approximation to y as a function of $x_1, x_2, \ldots, x_r$. Both parametric and nonparametric regression models are possible procedures for use [26–28]. However, when complex relationships between y and the x_js are present, it is likely that nonparametric procedures will be required in order to obtain a reasonable response surface approximation to y. If the response surface construction is carried out in a stepwise manner in which (i) the most important element of $\mathbf{x}$ with respect to the uncertainty in y is selected first (i.e., x_1) and the corresponding response surface constructed, (ii) then the next most important element of $\mathbf{x}$ with respect to the uncertainty in y is selected (i.e., x_2) and the corresponding response surface con-

UNCORRECTED PROOF

Please cite this article in press as: J.C. Helton et al., A sampling-based computational strategy for the representation ..., Comput. Methods Appl. Mech. Engrg. (2007), doi:10.1016/j.cma.2006.10.049

structed with x_1 and x_2, and (iii) this process continues until no more elements of $\mathbf{x}$ are determined to affect y, then this stepwise procedure also provides the sensitivity analysis results indicated in Step 4.

Step 6. Generate a "large" random sample from the uncertain inputs in consistency with the sampling distribution defined in Step 1 and use the response surface for y constructed in Step 5 to estimate y for each element of this sample. This creates a mapping between $x_1, x_2, \ldots, x_r$ and y of the form indicated in Eq. (2.25). However, unlike the mapping in Eq. (2.25), this mapping only involves the x_js that the sensitivity analysis in Step 4 identified as being important with respect to the uncertainty in y.

Step 7. Perform a sequential construction of the CBF, CCBF, CPF and CCPF for y with the response surface results from Step 6. In this sequential construction, a CBF, CCBF, CPF and CCPF are first estimated for y as indicated in Eqs. (2.21)–(2.24) with x_1 assigned its specified evidence space and $x_2, x_3, \ldots, x_r$ assigned degenerate evidence spaces (i.e., evidence spaces in which the sample space is given a basic probability assignment of one); then, a CBF, CCBF, CPF and CCPF are estimated for y as indicated in Eqs. (2.21)–(2.24) with x_1 and x_2 assigned their specified evidence spaces and $x_3, x_4, \ldots, x_r$ assigned degenerate evidence spaces; the process continues in this manner until the CBFs, CCBFs, CPFs and CCPFs for y no longer show meaningful change with the consideration of the specified evidence spaces for additional variables or the specified evidence spaces for all the variables identified in the sensitivity analysis performed at Step 5 (i.e., $x_1, x_2, \ldots, x_r$) have been incorporated into a CBF, CCBF, CPF and CCPF for y.

The indicated approach to the construction of CBFs, CCBFs, CPFs and CCPFs for model predictions has several desirable features, including (i) efficient use of model evaluations, (ii) capability to consider many different model predictions with the same set of model evaluations, (iii) mitigation of the dimensionality problem that hinders the propagation of evidence theory structures through a model when a large number of uncertain model inputs is under consideration, (iv) an "outside-in" approximation of CBFs, CCBFs, CPFs and CCPFs that always bounds the actual CBF, CCBF, CPF and CCPF for a model prediction (see Section 7, Ref. [29]), and (v) the capability to generate a variety of sensitivity analysis results.

4. Example for illustration

The example involves a system with two weak links (WLs) and two strong links (SLs) in an accident involving a fire that has the potential to result in a condition that could allow an unintended operation of the system [30] and is adapted from an example presented in Section 6 of Ref. [29]. The role of the SLs is to permit operation of the system only under intended conditions. The role of the WLs is to fail under accident conditions and thereby render the system incapable of operation. The failure of both SLs before the failure of either WL is considered to be the undesirable event as this places the system in a configuration in which an activating signal could result in operation of the system. The likelihood that such a configuration occurs is referred to as probability of loss of assured safety (PLOAS). The indicated probability (i.e., PLOAS) derives from the assumption that the exact temperatures at which the individual links will fail is not known precisely. Rather, there is assumed to be a random (i.e., aleatory) uncertainty resulting from manufacturing variability that determines the exact temperatures at which the individual links fail.

As described in Section 6 of Ref. [29] and formally derived in conjunction with Eq. (4.9) of Ref. [31], the value pF for PLOAS is given by

$$\mathrm{pF} = \sum_{k=1}^{2} \int_{\mathrm{TMNSL}_k}^{\mathrm{TMXSL}_k} \mathrm{fSL}_k(T_{\mathrm{SL}}) \times \left\{ \prod_{\substack{l=1 \\ l \neq k}}^{2} I[-\infty, \mathrm{TMPSL}_l[\mathrm{TMPSL}_k^{-1}(T_{\mathrm{SL}})], \mathrm{fSL}_l] \right\} \times \left\{ \prod_{j=1}^{2} I[\mathrm{TMPWL}_j[\mathrm{TMPSL}_k^{-1}(T_{\mathrm{SL}})], \infty, \mathrm{fWL}_j] \right\} \mathrm{d}T_{\mathrm{SL}}, \tag{4.1}$$

where (i) $\mathrm{TMPWL}_j(t)$ is the temperature (°C) of WL j at time t (min), (ii) $\mathrm{TMPSL}_k(t)$ is the temperature (°C) of SL k at time t (min), (iii) $\mathrm{TMPSL}_j(t)$ and $\mathrm{TMPSL}_k(t)$ are assumed to be increasing functions of time, (iv) $\mathrm{fWL}_j(T)$ is the density function (°C^{-1}) for failure temperature of WL j, (v) fSL_j is the density function (°C^{-1}) for failure temperature of SL k, (vi) time is assumed to range from $t\mathrm{MN}$ to $t\mathrm{MX}$ with $\mathrm{TMNSL}_k = \mathrm{TMPSL}_k(t\mathrm{MN})$ and $\mathrm{TMXSL}_k = \mathrm{TMPSL}_k(t\mathrm{MX})$, and (vii) $I[a, b, f] = \int_a^b f(T)\mathrm{d}T$ is used for notational convenience.

Further, the temperature curves and density functions in Eq. (4.1) are defined by

$$\mathrm{TMPWL}_j(t) = c_1 + [c_2 + c_{3j}\exp(-c_{4j}t)\sin(c_{5j}t)]\tanh(c_{6j}t) \tag{4.2}$$

$$\mathrm{TMPSL}_k(t) = c_1 + c_2\tanh[c_{62}(1 + c_{7k})t], \tag{4.3}$$

$$\mathrm{fWL}_j(T_{\mathrm{WL}}) = (1/c_9\sqrt{2\pi})\exp[-(T_{\mathrm{WL}} - c_8)^2/2c_9^2] \tag{4.4}$$

and

$$\mathrm{fSL}_k(T_{\mathrm{SL}}) = (1/c_{11}\sqrt{2\pi})\exp[-(T_{\mathrm{SL}} - c_{10})^2/2c_{11}^2] \tag{4.5}$$

with the indicated constraints defined in Table 1.

The 16 variables in Table 1 are assumed to be epistemically uncertain. For simplicity, it is assumed that the uncer-

UNCORRECTED PROOF

Table 1
Uncertain variables and associated uncertainty ranges considered in example uncertainty analyses

c_1 – Temperature (°C) of WLs and SLs before start of fire. Range: $[-30, 40\ °C]$.
c_2 – Temperature increase (°C) above c_1 at steady state. Range: $[800, 1000\ °C]$.
c_{31} – Peak amplitude of temperature transient for WL 1. Range: $[-2600, -100\ °C]$. c_{32} – Peak amplitude of temperature transient for WL 2. Range: $[-2600, -100\ °C]$.
c_{41} – Thermal heating time constant (min^{-1}) for WL 1. Range: $[0.2, 0.4\ min^{-1}]$. c_{42} – Thermal heating time constant (min^{-1}) for WL 2. Range: $[0.2, 0.4\ min^{-1}]$.
c_{51} – Frequency response (min^{-1}) of temperature transient for WL 1. Range: $[0.1, 0.2\ min^{-1}]$. c_{52} – Frequency response (min^{-1}) of temperature transient for WL 2. Range: $[0.1, 0.2\ min^{-1}]$.
c_{61} – Time constant (min^{-1}) determining the rate at which WL 1 reaches steady state temperature. Range: $[0.01, 0.015\ min^{-1}]$. c_{62} – Time constant (min^{-1}) determining the rate at which WL 2 reaches steady state temperature. Range: $[0.021, 0.025\ min^{-1}]$.
c_{71} – Factor (dimensionless) used to account for more rapid heating in SL 1 than in the associated WL (i.e., WL 2). Range: $[0.3, 0.5]$. c_{72} – Factor (dimensionless) used to account for more rapid heating in SL 2 than in the associated WL (i.e., WL 2). Range: $[0.6, 2.0]$.
c_8 – Expected value (°C) of normal distribution for WL failure temperatures. Range: $[285, 315\ °C]$.
c_9 – Standard deviation (°C) of normal distribution for WL failure temperatures. Range: $[4, 12\ °C]$.
c_{10} – Expected value (°C) of normal distribution for SL failure temperature. Range: $[560, 580\ °C]$.
c_{11} – Standard deviation (°C) of normal distribution for SL failure temperature. Range: $[15, 35\ °C]$.

Adapted from Table 1, Ref. [29].

Table 2
Illustrative specification of uncertainty information used in example uncertainty analyses with probability theory and evidence theory for variables in Table 1 (Table 2, Ref. [29])

Expert 1: States appropriate value for variable is in the interval $I_{11} = [a, b]$ but provides no information on uncertainty structure within $[a, b]$.
Expert 2: Divides $[a, b]$ into five nonoverlapping intervals of equal length (i.e., $I_{2i} = [a + (b - a)(i - 1)/5,\ a + (b - a)i/5)$ for $i = 1, 2, 3, 4$ and $I_{25} = [a + (b - a)(i - 1)/5,\ a + (b - a)i/5]$ for $i = 5$) and states that the appropriate value for the variable is equally likely to be in each of these intervals.
Expert 3: Divides $[a, b]$ into following five nonoverlapping intervals: $I_{31} = [a, a + (b - a)/10]$, $I_{32} = [a + (b - a)/10, a + 4(b - a)/10)$, $I_{33} = [a + 4(b - a)/10,\ a + 6(b - a)/10)$, $I_{34} = [a + 6(b - a)/10,\ a + 9(b - a)/10)$, $I_{35} = [a + 9(b - a)/10, b]$. States that the probability (i.e., likelihood) that the appropriate value for the variable is contained in each of these intervals is 0.05, 0.2, 0.5, 0.2 and 0.05, respectively.
Expert 4: Divides $[a, b]$ into following five nested intervals: $I_{41} = [a + 4(b - a)/10,\ a + 6(b - a)/10)$, $I_{42} = [a + 3(b - a)/10,\ a + 7(b - a)/10)$, $I_{43} = [a + 2(b - a)/10, a + 8(b - a)/10)$, $I_{44} = [a + (b - a)/10, a + 9(b - a)/10)$, $I_{45} = [a, b]$. States that amount of probability (i.e., likelihood) that can be assigned to the proposition that a given interval contains the appropriate value to use for the variable is 0.2.

tainty in each variable's possible values over the range indicated in Table 1 is specified in the same manner by four independent experts (Table 2).

The information in Table 2 is encoded into an evidence space representation for the epistemic uncertainty associated with each variable by interpreting the given probabilities as BPAs for the corresponding intervals (i.e., I_{11} for Expert 1, and I_{ij}, $j = 1, 2, \ldots, 5$ for Expert i, $i = 2, 3, 4$). Specifically, the BPA m_i associated with Expert i is given by

$$m_i(\mathcal{U}) = \begin{cases} \text{prob}_i(\mathcal{U}) & \text{if } \mathcal{U} \in \mathbb{E}_i \\ 0 & \text{otherwise} \end{cases} \tag{4.6}$$

for an arbitrary set $\mathcal{U}$ of points from $[a, b]$, where $\mathbb{E}_1 = \{I_{11}\}$ and $\mathbb{E}_i = \{I_{ij}, j = 1, 2, \ldots, 5\}$ for $i = 2, 3, 4$. The BPAs from the individual experts are then equally weighted to produce a final BPA m given by

$$m(\mathcal{U}) = \sum_{i=1}^{nE} m_i(\mathcal{U}) \Big/ nE, \tag{4.7}$$

where $nE = 4$ is the number of experts and $\mathcal{U}$ is an arbitrary subset of points from $[a, b]$. The preceding procedure results in an evidence space with 13 focal elements for each

Table 3
Basic probability assignments (BPAs) for a Variable on the interval $[a, b]$ derived from the information in Table 2 (Table 3, Ref. [29])

$m(\mathcal{U}) = 3/10$ if $\mathcal{U} = I_1 = [a, b]$
$= 1/20$ if $\mathcal{U} = I_2 = [a, a + (b - a)/5)$
$= 1/20$ if $\mathcal{U} = I_3 = [a + (b - a)/5, a + 2(b - a)/5)$
$= 9/40$ if $\mathcal{U} = I_4 = [a + 2(b - a)/5, a + 3(b - a)/5)$
$= 1/20$ if $\mathcal{U} = I_5 = [a + 3(b - a)/5, a + 4(b - a)/5)$
$= 1/20$ if $\mathcal{U} = I_6 = [a + 4(b - a)/5, b]$
$= 1/80$ if $\mathcal{U} = I_7 = [a, a + (b - a)/10)$
$= 1/20$ if $\mathcal{U} = I_8 = [a + (b - a)/10, a + 4(b - a)/10)$
$= 1/20$ if $\mathcal{U} = I_9 = [a + 6(b - a)/10, a + 9(b - a)/10)$
$= 1/80$ if $\mathcal{U} = I_{10} = [a + 9(b - a)/10, b]$
$= 1/20$ if $\mathcal{U} = I_{11} = [a + 3(b - a)/10, a + 7(b - a)/10)$
$= 1/20$ if $\mathcal{U} = I_{12} = [a + 2(b - a)/10, a + 8(b - a)/10)$
$= 1/20$ if $\mathcal{U} = I_{13} = [a + (b - a)/10, a + 9(b - a)/10)$
$= \frac{0}{1.0}$ otherwise

UNCORRECTED PROOF

Please cite this article in press as: J.C. Helton et al., A sampling-based computational strategy for the representation ..., Comput. Methods Appl. Mech. Engrg. (2007), doi:10.1016/j.cma.2006.10.049

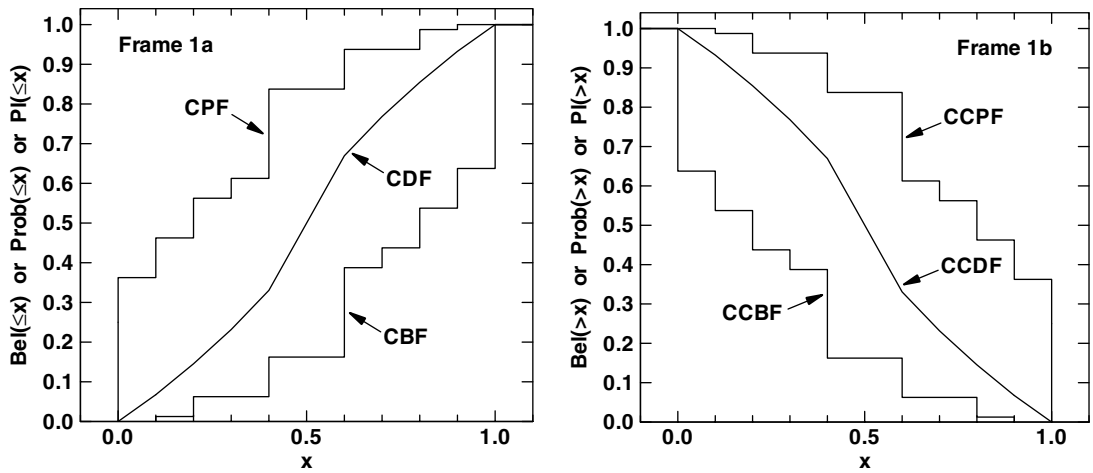

Fig. 1. Form of the CPF, CDF, CBF, CCPF, CCDF and CCBF that results for each variable from the uncertainty information in Table 2 with variable range normalized to [0, 1].

variable in Table 1 (Table 3). In turn, a probability distribution for use in sampling can be defined for each variable as indicated in Eq. (2.26). The form of the CPF, CDF, CBF, CCPF, CCDF and CCBF that results for each variable is shown in Fig. 1.

5. Example results

For this example,

$$\mathbf{x} = [x_1, x_2, \ldots, x_{16}] = [c_1, c_2, c_{31}, \ldots, c_{11}] \tag{5.1}$$

corresponds to the $nX = 16$ variables in Table 1. Further, the dependent variables selected for possible analysis correspond to

$$\begin{aligned}\mathbf{y} &= [y_1, y_2, \ldots, y_5] \\ &= [\mathrm{WL1T25}, \mathrm{WL1T75}, \mathrm{SL1T25}, \mathrm{SL1T75}, \mathrm{pF}],\end{aligned} \tag{5.2}$$

where (i) WL1T25 and WL1T75 are the temperatures of WL 1 at 25 and 75 min, respectively (see Eq. (4.2)), (ii) SL1T25 and SL1T75 are defined similarly for SL 1 (see Eq. (4.3)) and (iii) pF is the PLOAS (see Eq. (4.1)). Given the time dependency of the results and the presence of multiple WLs and SLs, a real analysis would probably consider many more uncertain results than the five indicated above. The individual steps in the computational strategy for estimating CBFs, CCBFs, CPFs and CCPFs for model results are now illustrated.

5.1. Step 1: define sampling distribution

The sampling distribution for each uncertain variable was defined as shown in Eq. (2.26). Specifically, this results in a distribution with a density function defined by

$$d_j(x_j) = \sum_{k=1}^{13} \delta(x_j|I_k)m(I_k)/L(I_k), \tag{5.3}$$

where I_k and $m(I_k)$ are defined in Table 3, $L(I_k)$ is the length of the interval I_k, and the indicator variable $\delta(x_j \mid I_k)$ is defined in conjunction with Eq. (2.26). The form of the CDF and CCDF associated with this distribution is shown in Fig. 1.

5.2. Step 2: generate Latin hypercube sample

A Latin hypercube sample [9,10]

$$\mathbf{x}_i = [x_{i1}, x_{i2}, \ldots, x_{i,16}], \quad i = 1, 2, \ldots, nS, \tag{5.4}$$

of size $nS = 200$ was generated from the possible values for $\mathbf{x}$ in consistency with the distributions defined by the density functions in Eq. (5.3). Further, the Iman/Conover restricted pairing technique was used in the generation of this sample to assure that no spurious correlations between the sampled variables were present [32].

5.3. Step 3: propagate sample through model

The model was evaluated for each element of the sample in Eq. (5.4). This produced the mapping

$$[\mathbf{x}_i, \mathbf{y}_i] = [\mathbf{x}_i,\ \mathrm{WL1T25}_i, \mathrm{WL1T75}_i, \mathrm{SL1T25}_i, \mathrm{SL2T75}_i, \mathrm{pF}_i] \tag{5.5}$$

for $i = 1, 2, \ldots, nS = 200$ from uncertain inputs to uncertain results. As shown in Fig. 2, the analysis actually produced time-dependent values for the WL and SL temperatures. Such time-dependence is typical of the results obtained in large analyses. The values for the temperature results in Eq. (5.5) correspond to the results associated with vertical lines drawn through the time–temperature curves in Fig. 2 at times of 25 and 75 min. The values for pF in Eq. (5.5) are summarized by the CCDF in Fig. 3.

5.4. Step 4: perform sensitivity analysis

This step involves carrying out a sensitivity analysis to determine the dominant contributions to the uncertainty

UNCORRECTED PROOF

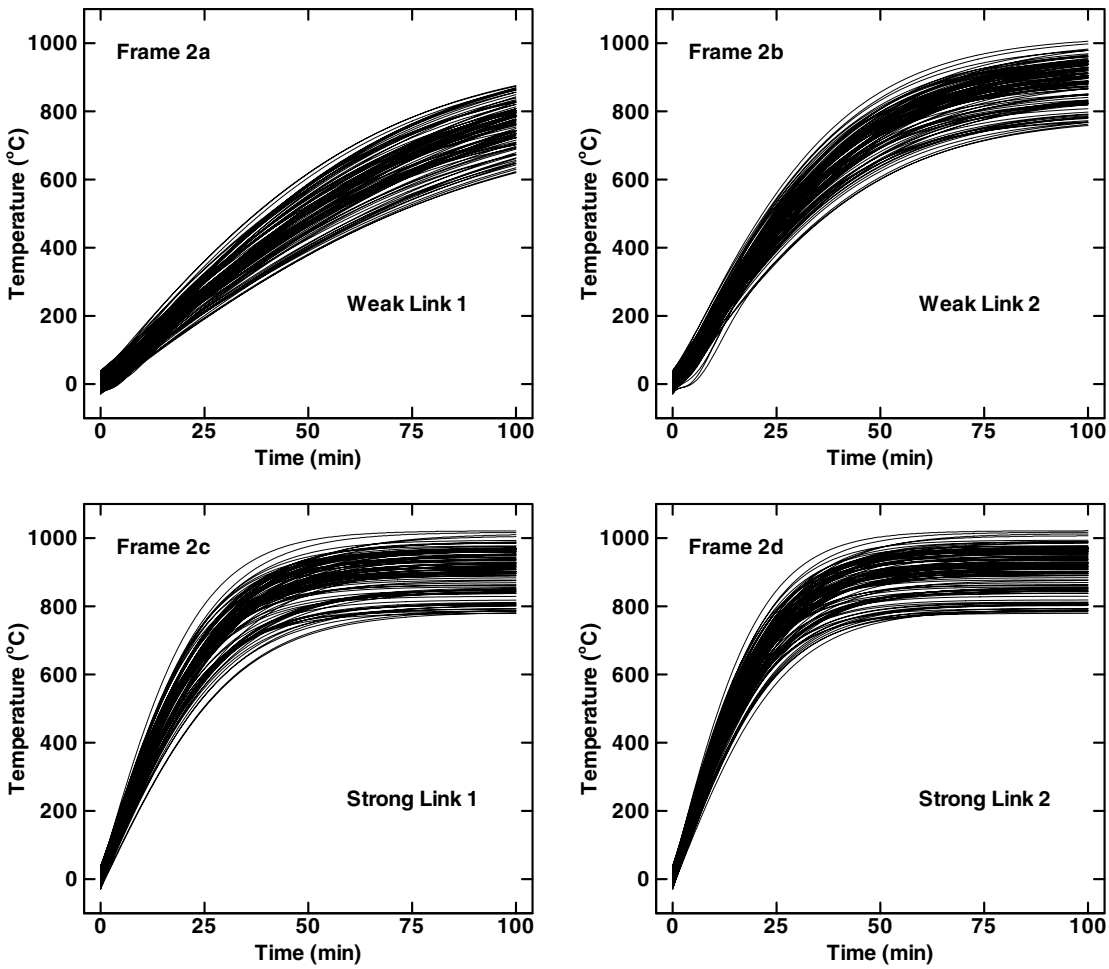

Fig. 2. Time-dependent curves for WLs and SLs obtained with Latin hypercube sample with 100 curves from sample of size 200 shown.

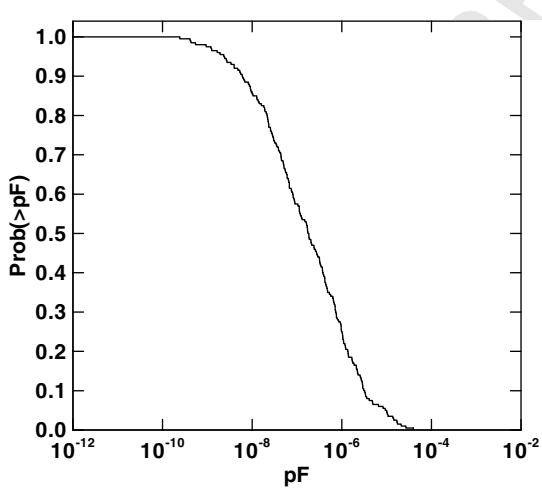

Fig. 3. Values for pF obtained with Latin hypercube sample of size 200 shown as CCDF.

in each element of **y**. This analysis is based on exploring the mapping between analysis inputs and analysis results in Eq. (5.5). Many procedures exist that might be used in this exploration, including correlation and partial correlation analysis with raw or rank-transformed data, linear regression analysis with raw or rank-transformed data, statistical tests for patterns based on gridding, entropy tests for patterns based on gridding, squared rank differences/rank correlation test, two dimensional Kolmogorov–Smirnov test, and tests for patterns based on distance measures [8].

For illustration, the results of a sensitivity analysis with stepwise rank regression are presented in Table 4, with variable importance indicated by order of selection in the stepwise procedure, the absolute value of the standardized rank regression coefficients (SRRCs) in the final regression model, and incremental changes in R^2 values as additional variables are added to the model (see Section 6.6.6, Ref. [33], for a discussion of sensitivity analysis with rank regression). For example, the three dominant variables contributing to the uncertainty in WL1T25 are c_{61}, c_1 and c_2.

5.5. Step 5: develop response surface approximation

This step involves developing response surface replacements for the original model with the variables identified as being important in Step 4. Possibilities for response surface construction include parametric regression procedures such as linear regression (LIN_REG) and quadratic regres-

Table 4
Sensitivity analysis based on stepwise rank regression for mapping $[\mathbf{x}_i, \mathbf{y}_i], y = 1, 2, \ldots, nS = 200$, in Eq. (5.5)

Var[a]	SRRC[b]	R^{2c}
WL1T25: WL 1 temperature at 25 min		
c_{61}	0.71	0.54
c_1	0.49	0.78
c_2	0.42	0.96
SL1T25: SL 1 temperature at 25 min		
c_2	0.70	0.52
c_{62}	0.43	0.72
c_{71}	0.33	0.83
c_1	0.33	0.93
c_{31}	0.05	0.94
WL1T75: WL 1 temperature at 75 min		
c_{61}	0.64	0.46
c_2	0.64	0.87
c_1	0.30	0.96
SL1T75: SL 1 temperature at 75 min		
c_2	0.94	0.89
c_1	0.30	0.97
c_{71}	0.03	0.97
log(pF): Logarithm PLOAS		
c_{71}	0.67	0.47
c_2	0.38	0.62
c_1	−0.29	0.70
c_{72}	0.23	0.76
c_8	0.20	0.80
c_9	0.19	0.83
c_{10}	−0.16	0.85
c_{11}	0.16	0.88
c_{42}	−0.14	0.90
c_{32}	−0.11	0.91
c_{62}	0.11	0.92
c_{52}	−0.10	0.93

[a] Variables listed in order of selection in stepwise process with variable required to have an α-values of 0.02 and 0.05 to enter and be retained in the regression, respectively.
[b] Standardized rank regression coefficient (SRRC) for variable in final regression model.
[c] Cumulative R^2-value with entry of each variable into the regression model.

sion (QUAD_REG) and nonparametric regression procedures such as locally weighted regression (LOESS), generalized additive models (GAMs), projection pursuit regression (PP_REG) and multivariate adaptive regression splines (MARS). Brief descriptions and additional background references for LIN_REG, QUAD_REG, LOESS, GAMs and PP_REG are given in Refs. [26–28]. A description of the MARS procedure is given in Ref. [34].

The preceding procedures can all be carried out in a stepwise manner to determine variable importance, with (i) the most important variable $\tilde{x}_1$ being the variable that results in the single-variable model with the most predictive capability, (ii) the second most important variable $\tilde{x}_2$ being the variable that in conjunction with $\tilde{x}_1$ results in the two-variable model with the most predictive capability, and so on until (iii) some stopping criterion is reached that indicates that the consideration of additional variables does not produce models with improved predictive capability. Order of selection in the stepwise construction process and fraction of variability explained (i.e., an R^2-value) can be used to indicate variable importance. The f-statistic with appropriate degrees of freedom (see Section 3.9, Ref. [35], and Section 3.13, Ref. [36]) can be used to determine a stopping point in the stepwise variable selection procedure. Additional discussion of nonparametric regression is available in a number of texts [35–40].

If the number of elements in $\mathbf{x}$ is not excessively large, then this construction can be carried out in a stepwise manner analogous to that shown in Table 4 for stepwise rank regression. The most efficient procedure is to consider only the variables identified in Step 4 as being important. However, if computationally practicable, this construction can be carried out with sequential stepwise consideration of all components of $\mathbf{x}$ as candidates for inclusion in the response surface under consideration. Then, as indicated in the description of Step 5 in Section 3, the sensitivity analysis in Step 4 and the response surface construction in Step 5 are in effect being carried out together, with variable importance indicated by order of selection in the stepwise response surface construction and the corresponding changes in incremental R^2 values.

For illustration, summaries of stepwise response surface construction with several different methods are presented in Table 5 for log(pF). As the MARS procedure worked as well as or better than the other response surface procedures considered for constructing approximations to the elements of $\mathbf{y}$, the MARS procedure was selected for use in determining the response surface approximations to be employed in constructing evidence theory results in Step 6 (see Table 5 for log(pF) and Table 6 for WL1T25, WL1T75, SL1T25 and SL1T75). The biggest differences in the response surface constructions for the different procedures occurred for log(pF) (Table 5). The results with the procedures illustrated for log(pF) in Table 5 are very similar for WL1T25, WL1T75, SL1T25 and SL1T75 as a result of the smooth and well-defined relationships between these variables and the elements of $\mathbf{x}$. However, such similarity should not always be expected to be the case.

The high R^2 values for the final response surface constructions with the MARS procedure in Tables 5 and 6 are indicative of a high predicative capability. As a further test, a "leave one out" analysis was carried out in which one observation at a time was dropped from the mapping in Eq. (5.5) and then MARS response surfaces were constructed from the remaining 199 observations and used to predict the elements of the dropped $\mathbf{y}$-value. For each element y of $\mathbf{y}$, the result is a sequence

$$[y_i, \hat{y}_i], \quad i = 1, 2, \ldots, nS = 200, \tag{5.6}$$

where y_i is the original value in Eq. (5.5) and $\hat{y}_i$ is the corresponding predicted value. As shown by the scatterplots for the observed and predicted values for WL1T75 and log(pF) in Fig. 4, the MARS procedure is predicting quite well, although there is some noise in the predictions for log(pF). Comparisons similar to the comparison for

UNCORRECTED PROOF

Table 5
Summaries of stepwise construction of response surface approximations of log(pF) from mapping in Eq. (5.5)

Var[a]	R^{2b}	d.f.[c]	p-val[d]	PRESS[e]
LIN_REG				
c_{71}	0.4674	1.0	0.0000	1.24E2
c_2	0.6220	1.0	0.0000	8.93E1
c_1	0.7005	1.0	0.0000	7.16E1
c_{72}	0.7624	1.0	0.0000	5.74E1
c_9	0.8076	1.0	0.0000	4.68E1
c_8	0.8464	1.0	0.0000	3.79E1
c_{11}	0.8766	1.0	0.0000	3.07E1
c_{10}	0.9011	1.0	0.0000	2.48E1
c_{42}	0.9234	1.0	0.0000	1.96E1
c_{52}	0.9359	1.0	0.0000	1.66E1
c_{62}	0.9463	1.0	0.0000	1.41E1
c_{32}	0.9565	1.0	0.0000	1.17E1
LOESS				
c_{71}	0.4674	1.0	0.0000	1.24E2
c_2	0.6681	12.3	0.0000	8.83E1
c_{72}	0.6853	−10.1	0.0000	7.53E1
c_1	0.7629	1.3	0.0000	5.76E1
c_8	0.8038	1.5	0.0000	4.86E1
RS_REG				
c_{71}	0.4727	2.0	0.0000	1.24E2
c_2	0.6260	3.0	0.0000	9.15E1
c_1	0.7089	4.0	0.0000	7.43E1
c_{72}	0.7759	5.0	0.0000	6.08E1
c_9	0.8291	6.0	0.0000	4.90E1
c_8	0.8704	7.0	0.0000	4.14E1
c_{42}	0.9030	8.0	0.0000	3.60E1
c_{11}	0.9340	9.0	0.0000	2.73E1
c_{10}	0.9610	10.0	0.0000	1.89E1
c_{32}	0.9737	11.0	0.0000	1.65E1
c_{52}	0.9869	12.0	0.0000	9.03E0
c_{62}	0.9970	13.0	0.0000	3.03E0
GAM				
c_{71}	0.4675	1.0	0.0000	1.24E2
c_2	0.6349	4.0	0.0000	8.90E1
c_1	0.7104	1.0	0.0000	7.13E1
c_{72}	0.7722	1.0	0.0000	5.67E1
c_9	0.8178	2.0	0.0000	4.60E1
c_8	0.8579	2.0	0.0000	3.68E1
c_{11}	0.8949	7.0	0.0000	2.92E1
c_{10}	0.9177	2.0	0.0000	2.32E1
c_{42}	0.9416	2.0	0.0000	1.71E1
c_{32}	0.9498	1.0	0.0000	1.50E1
c_{62}	0.9591	2.0	0.0000	1.24E1
c_{52}	0.9678	2.0	0.0000	1.01E1
MARS				
c_{71}	0.4674	1.0	0.0000	1.24E2
c_2	0.6220	1.0	0.0000	9.44E1
c_1	0.7110	2.0	0.0000	7.19E1
c_{72}	0.7776	2.0	0.0000	5.93E1
c_9	0.8267	2.0	0.0000	5.08E1
c_{42}	0.8857	6.0	0.0000	4.87E1
c_8	0.8990	−1.0	0.0000	3.35E1
c_{11}	0.9393	6.0	0.0000	2.55E1
c_{10}	0.9597	1.0	0.0000	2.30E1
c_{52}	0.9755	8.0	0.0000	1.98E1
c_{32}	0.9891	11.0	0.0000	1.13E1
c_{62}	0.9971	9.0	0.0000	3.99E0
c_{31}	0.9978	9.0	0.0000	4.36E0

Table 5 (*continued*)

Var[a]	R^{2b}	d.f.[c]	p-val[d]	PRESS[e]
PP_REG				
c_{71}	0.4696	1.3	0.0000	1.26E2
c_2	0.6500	5.6	0.0000	8.67E1
c_{72}	0.7373	7.4	0.0000	8.57E1
c_{42}	0.8196	16.2	0.0000	7.57E1
c_9	0.8890	19.3	0.0000	7.95E1
c_{10}	0.9278	8.0	0.0000	6.14E1

[a] Variables listed in order of selection in stepwise process.
[b] Cumulative R^2-value with entry of each variable into the model.
[c] Incremental degrees of freedom with entry of each variable into the model.
[d] p-Value associated with entry of each variable into the model.
[e] Predicted error sum of squares (PRESS) value for model; a deviation from monotonically decreasing PRESS values indicates that the model may be overfitting the data.

Table 6
Summaries of stepwise construction of response surface approximations to WL1T25, WL5T75, SL1T25 and SL1T75 from mapping in Eq. (5.5) with the MARS procedure

Var[a]	R^{2b}	d.f.[c]	p-val[d]	PRESS[e]
WL1T25: WL 1 temperature at 25 min				
c_{61}	0.5946	4.0	0.0000	1.12E5
c_1	0.8283	2.0	0.0000	4.83E4
c_2	0.9998	−1.0	0.0000	5.44E1
c_{41}	0.9999	4.0	0.0000	2.66E1
c_{51}	1.0000	8.0	0.0000	2.00E1
c_{31}	1.0000	9.0	0.0000	4.89E0
SL1T25: SL 1 temperature at 25 min				
c_2	0.5699	2.0	0.0000	2.37E5
c_{62}	0.7700	2.0	0.0000	1.29E5
c_{71}	0.8849	0.0	0.0000	6.27E4
c_1	1.0000	17.0	0.0000	3.17E0
WL1T75: WL 1 temperature at 75 min				
c_{61}	0.5550	5.0	0.0000	3.44E5
c_2	0.9176	0.0	0.0000	6.05E4
c_1	1.0000	13.0	0.0000	2.60E0
SL1T75: SL 1 temperature at 75 min				
c_2	0.8947	2.0	0.0000	6.44E4
c_1	0.9969	0.0	0.0000	1.86E3
c_{62}	0.9987	3.0	0.0000	8.60E2
c_{71}	1.0000	11.0	0.0000	1.72E0

[a] Variables listed in order of selection in stepwise process.
[b] Cumulative R^2-value with entry of each variable into the model.
[c] Incremental degrees of freedom with entry of each variable into the model.
[d] p-value associated with entry of each variable into the model.
[e] Predicted error sum of squares (PRESS) value for model; a deviation from monotonically decreasing PRESS values indicates that the model may be overfitting the data.

WL1T75 were also obtained for WL1T25, SL1T25 and SL2T75.

5.6. Step 6: approximate y for large random sample

A random sample

$$\mathbf{x}_i = [x_{i1}, x_{i2}, \ldots, x_{i,16}], \quad i = 1, 2, \ldots, nS, \tag{5.7}$$

UNCORRECTED PROOF

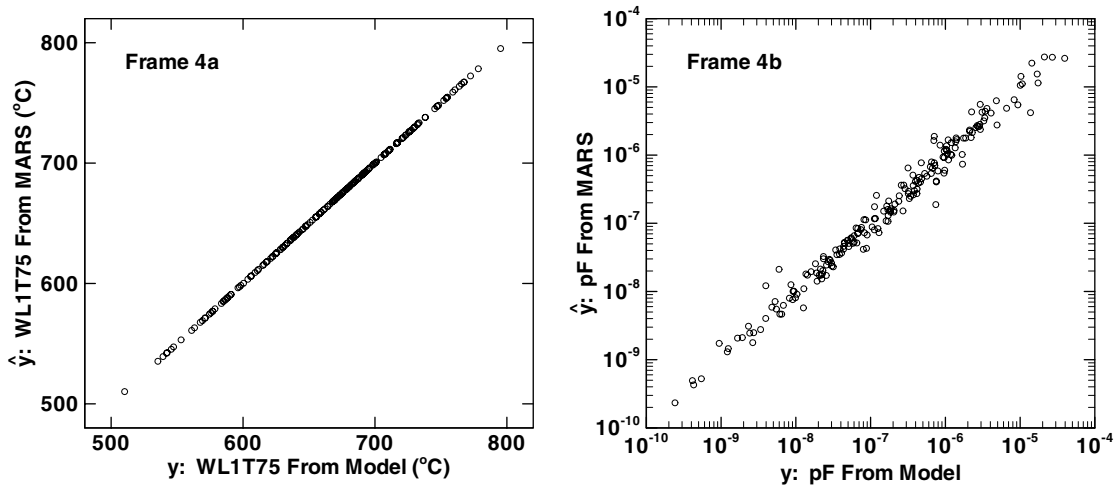

Fig. 4. Comparison of observed values (i.e., y as indicated in Eq. (5.6)) and MARS response surface predicted values (i.e., $\hat{y}$ as indicated in Eq. (5.6)): (a) WL1T75, and (b) log(pF).

of size $nS = 10^6$ was generated from the possible values for $\mathbf{x}$ in consistency with the distributions defined by the density functions in Eq. (5.3). The corresponding value $\hat{\mathbf{y}}_i$ for $\mathbf{y}_i$ was then estimated for each element of this sample with the MARS approximations to WL1T25, WL1T75, SL1T25, SL1T75 and log(pF) indicated in Tables 5 and 6. This created the mapping

$$[\mathbf{x}_i, \hat{\mathbf{y}}_i], \quad i = 1, 2, \ldots, nS = 10^6, \tag{5.8}$$

for use in estimating evidence theory results for the elements of $\mathbf{y}$.

5.7. Step 7: approximate evidence space results

The approximation of evidence space results is illustrated for WL1T25, WL1T75, SL1T25, SL1T25 and log(pF) for the construction of CCBFs, CCDFs and CCPFs as indicated in Eqs. (2.22), (2.4) and (2.24). The construction of CBFs, CDFs and CPFs is similar (see Eqs. (2.21), (2.3) and (2.23)). For comparison, results were obtained with both the MARS response surfaces for WL1T75 and log(pF) and the actual values for WL1T75 and log(pF). Such a comparison would not be possible in a real analysis with computationally demanding models but is possible here because the example model/analysis is inexpensive to evaluate.

The results for WL1T75 are shown in Fig. 5, with the results obtained from the response surface approximation shown in the left frame and the results obtained from the actual model predictions shown in the right frame. The outermost CCBFs and CCPFs in the two frames were obtained with the most important variable (i.e., c_{61}; see Table 6) assigned its original evidence space and the remaining variables assigned degenerate evidence spaces.

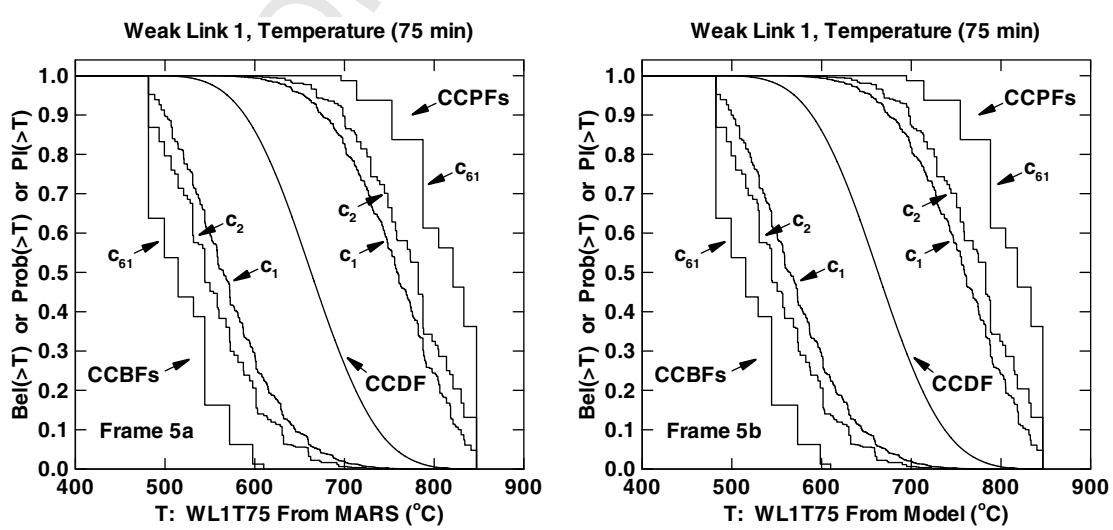

Fig. 5. Stepwise construction of CCBFs and CCPFs for WL1T75 with c_{61}, c_2 and c_1: (a) construction with MARS response surface approximation to WL1T75 (left frame), and (b) construction with predicted values for WL1T75 (right frame).

Thus, these CCBFs and CCPFs were constructed from an evidence space for **x** with 13 focal elements (see Table 3). Then, the next inner CCBFs and CCPFs were obtained with c_{61} and the next most important variable (i.e., c_2; see Table 6) assigned their original evidence spaces and the remaining variables assigned degenerate evidence spaces, with the result that the CCBFs and CCPFs are now being constructed from an evidence space with $13^2 = 169$ focal elements. The process continues similarly with the addition of c_1 in the next iteration and the corresponding consideration of an evidence space with $13^3 = 2197$ focal elements. The process stops at this point as c_{61}, c_2 and c_1 are the only variables identified as affecting WL1T75. The CCDFs that result from the distribution defined by the density functions in Eq. (5.3) are also shown in Fig. 5, with these CCDFs appearing between the CCBFs and the CCPFs as should be the case. As comparison of the left and right frames in Fig. 5 shows, the CCBFs and CCPFs obtained from the MARS response surface approximation are effectively the same as those obtained from the actual model predictions.

The evidence space results for WL1T25, SL1T25 and SL1T75 are similar to those for WL1T75 (Fig. 6). The results for WL1T25 and SL1T75 illustrate the negligible changes in CCBFs and CCPFs that take place when variables that have little effect on the result of interest are included in the construction process. As indicated in Table 6, c_{41} has little effect on WL1T25 and c_{62} has little effect on SL1T75. As a result, their inclusion in the CCBFs and CCPFs for WL1T25 and SL1T75, respectively, has little impact on the estimates for these outcomes.

The results for log(pF) are shown in Fig. 7, with the results obtained from the MARS response surface approximation shown in the left frames and the results obtained from the actual model predictions shown in the right frames. The construction procedure is the same as previously illustrated in Fig. 5 for WL1T75. The pF axis is ter-

PROOF

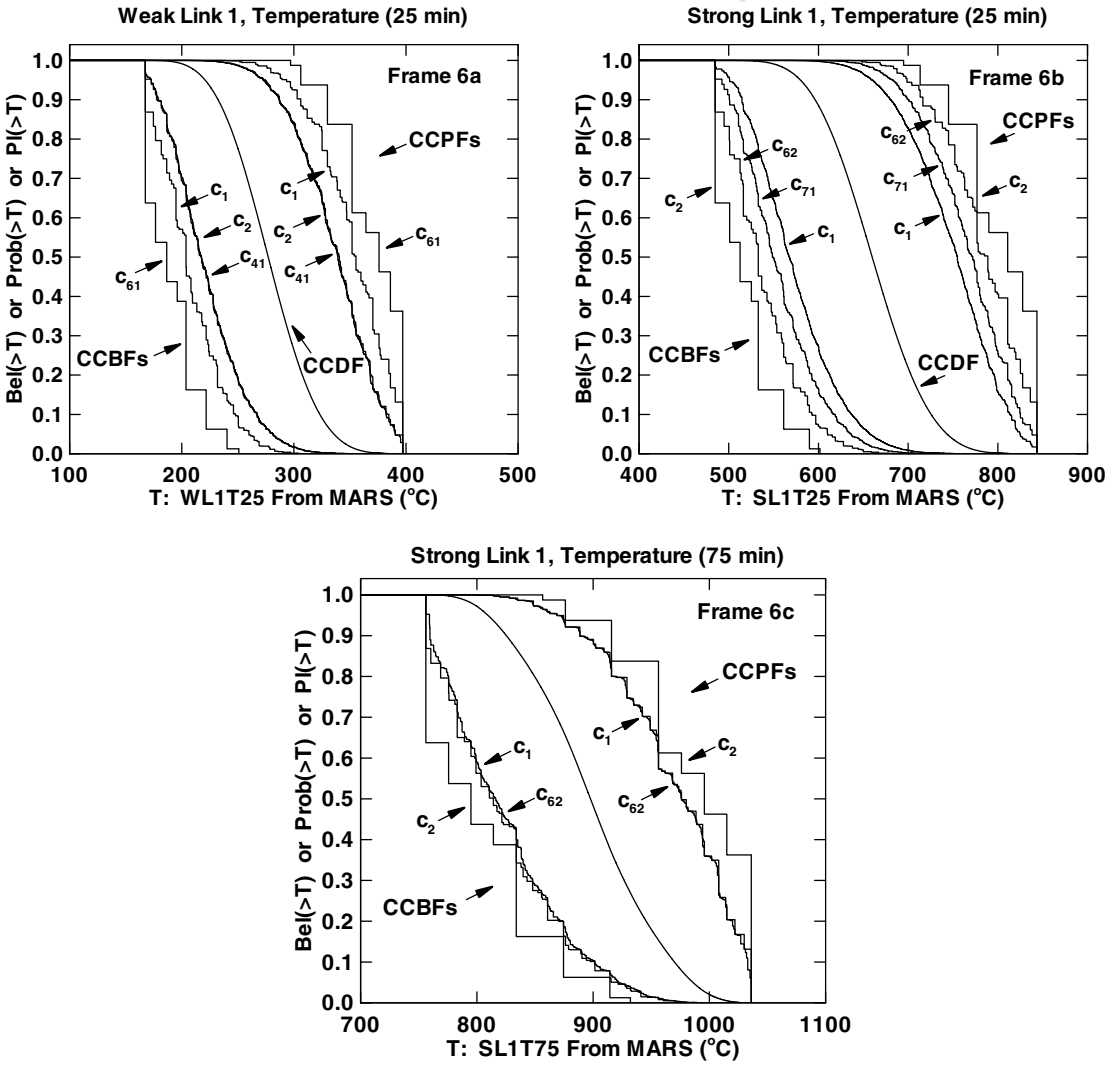

Fig. 6. Stepwise construction of CCBFs and CCPFs with MARS response surface approximations for WL1T25, SL1T25 and SL1T75: (a) WL1T25 with c_{61}, c_1, c_2 and c_{41}, (b) SL1T25 with c_2, c_{62}, c_{71} and c_1, and (c) SL1T75 with c_2, c_1 and c_{62}.

Please cite this article in press as: J.C. Helton et al., A sampling-based computational strategy for the representation ..., Comput. Methods Appl. Mech. Engrg. (2007), doi:10.1016/j.cma.2006.10.049

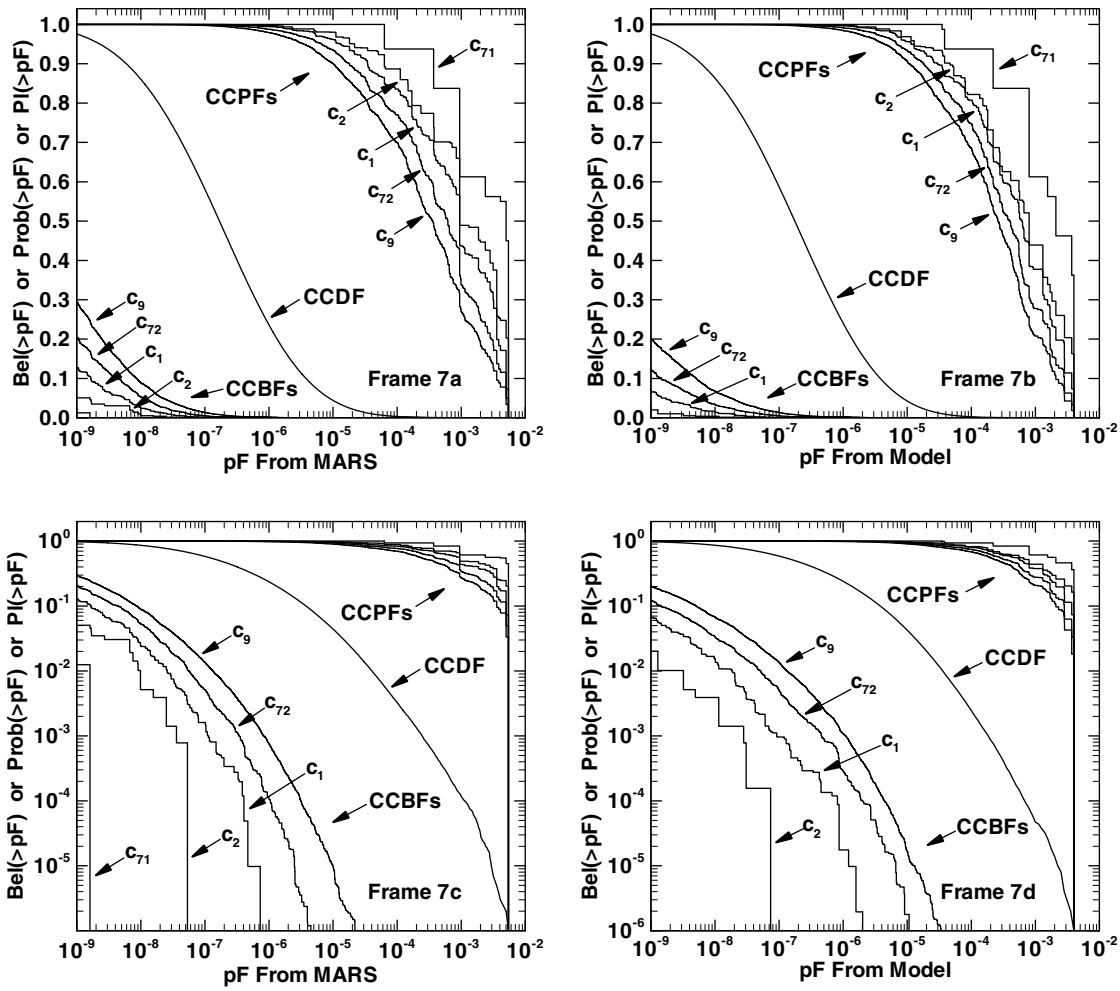

Fig. 7. Stepwise construction of CCBFs and CCPFs for pF with c_{71}, c_2, c_1, c_{72} and c_9 (a, c) construction with MARS response surface approximation to log(pF) (left frames), and (b, d) construction with predicted values for log(pF) (right frames).

minated at 10^{-9} for two reasons. First, the original Latin hypercube sample used in response surface construction only resulted in values for pF down to $10^{-9.6}$; thus, values for pF much less than 10^{-9} will involve results based on extrapolation rather than interpolation. Second, it is difficult to give much credence to probabilities less than 10^{-9} other than to acknowledge that they are "small." Because of the small values associated with the CCBFs, results are shown with both a linear scale (upper two frames) and a log scale (lower two frames) on the ordinate (i.e., the belief, probability and plausibility axis).

The constructions of the CCBFs and CCPFs in Fig. 7 sequentially involves 1–5 variables (i.e., c_{71}, c_2, c_1, c_{72} and c_9 in sequence; see Table 5). The corresponding evidence spaces have 13^k, $k = 1, 2, 3, 4, 5$, focal elements, with $13^5 =$ 371,293 focal elements in the evidence space for $\mathbf{x}$ when all five variables have their original evidence spaces and degenerate evidence spaces are assigned to the remaining variables. As indicated by the separation of the CCBFs and CCPFs obtained for 4 and 5 variables, the CCBFs and CCPFs in Fig. 7 are probably not fully converged to their true values. This lack of convergence is consistent with the MARS response surface for log(pF) with the indicated 5 variables having an R^2-value of 0.83 (Table 5). Thus, approximately 17% of the uncertainty in log(pF) is not captured by the response surface approximation in use.

One possibility is to continue the sequential construction of CCBFs and CCPFs by adding a sixth variable (i.e., c_{42}, which would increase the R^2-value for the MARS response surface to 0.89; see Table 5). This would bring a inward shift of the CCBFs and CCPFs but at the computational cost associated with increasing the number of focal elements in the evidence space for $\mathbf{x}$ from 13^5 to $13^6 = 4{,}826{,}809$. At this point, the sample of size $nS = 10^6$ in Eq. (5.7) may not be sufficiently large to assure adequate coverage of this many focal elements. In particular, there must be enough observations from each focal element to provide an approximate estimate of the minimum and maximum of the variable under consideration (i.e., log(pF) in this case) on each focal element. However, it is important to recognize that the sample size does not necessarily have to be substantially larger than the number of focal elements when there is significant overlap of the focal elements.

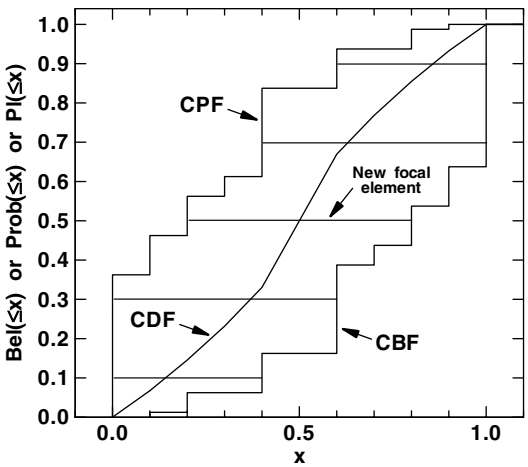

Fig. 8. Simplification of an evidence space with each horizontal line corresponding to a focal element with a BPA of 0.2 in a new evidence space.

Several possibilities exist at this point. One is to conclude that an adequate bound on the location of the true CCBF and CCPF has been determined and that the analysis can be terminated. In particular, the construction process is "outside-in" in the sense that the true CCBF and CCPF that results from a full consideration of the evidence spaces for all elements of **x** will always lie inside the constructed CCBFs and CCPFs (see Section 7, Ref. [29]). The preceding statement is conditional on two assumptions: (i) that the response surface in use is a "good" approximation to the result under consideration, and (ii) that a sufficiently large sample has been used to obtain converged estimates for the CCBF and CCPF for the reduced evidence space.

Another possibility is to pay the computational cost and keep adding variables until convergence is achieved. This could result in having to increase the size of the sample in Eq. (5.7). For log(pF), this could mean considering a total of nine variables, which would bring the R^2-value for the MARS response surface approximation up to 0.96 (i.e., with inclusion of $c_{71}, c_2, c_1, c_{72}, c_9, c_{42}, c_8, c_{11}, c_{10}$; see Table 5). However, at the end of the analysis, this entails considering an evidence space for **x** that involves 13^9 focal elements.

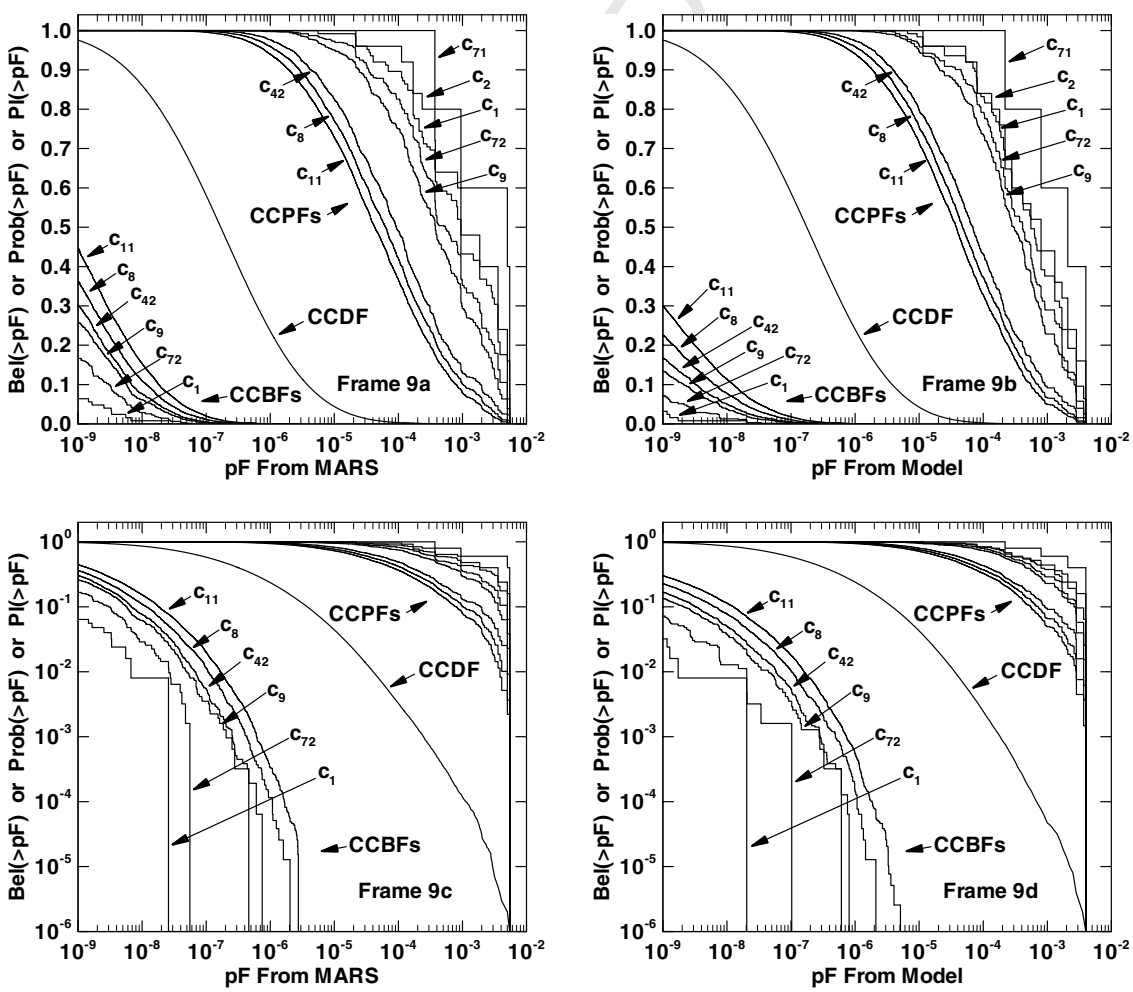

Fig. 9. Stepwise construction of CCBFs and CCPFs for pF with the evidence spaces for the individual components of **x** redefined to have five focal elements as indicated in conjunction with Fig. 8 and sequential inclusion of $c_{71}, c_2, c_{11}, c_{72}, c_9, c_{42}, c_8$ and c_{11}: (a) construction with MARS response surface approximation to log(pF) (left frames), and (b, d) construction with predicated values for log(pF) (right frames).

Yet another possibility is to simplify the analysis by reducing the complexity of the evidence spaces associated with the elements of **x**. In particular, approximations to the original evidence spaces can be defined that involve fewer focal elements but still capture the general nature of the original uncertainty characterization. This can be done on the basis of focal elements defined by horizontal lines drawn between the CPF and CBF for a variable (Fig. 8). In particular, the horizontal lines in Fig. 8 can be viewed as defining focal elements that correspond to the intervals [0.0, 0.4], [0.0, 0.6], [0.2, 0.8], [0.4, 1.0] and [0.6, 1.0] and have BPAs of 0.2. The result is a new and simpler evidence space for the variable that now has 5 rather than 13 focal elements. In general, the appropriate simplification would depend on the structure of the original evidence space, the amount of desired or necessary simplification, and the importance of the variable. In particular, it might be desirable to impose less simplification on the more important variables and more simplification on the less important variables.

As an example, the analysis for log(pF) was carried out with the evidence spaces for the individual components of **x** redefined to have five focal elements as indicated in conjunction with Fig. 8. This resulted in the need to consider sequential evidence spaces for **x** with fewer focal elements than used in the construction of the CCBFs and CCPFs in Fig. 7 and, as a result, allowed the incorporation of the effects of more components of **x** into the final CCBF and CCPF for log(pF). Although the uncertainty in the individual components of **x** has increased because of the reduction of the number of focal elements from 13 to 5, the estimated uncertainty in log(pF) has actually decreased because of the use of more components of **x** in the construction of the final CCBF and CCPF (i.e., compare final CCBFs and CCPFs in Figs. 7 and 9). Thus, although conservative due to the reduction in the number of focal elements, the final CCBF and CCPF in Fig. 9 provides a better representation of the uncertainty in log(pF) than the final CCBF and CCPF in Fig. 7.

The results in Fig. 9 produced a surprise in that the effect of c_{42} on the location of the CCPF is greater than its incre-

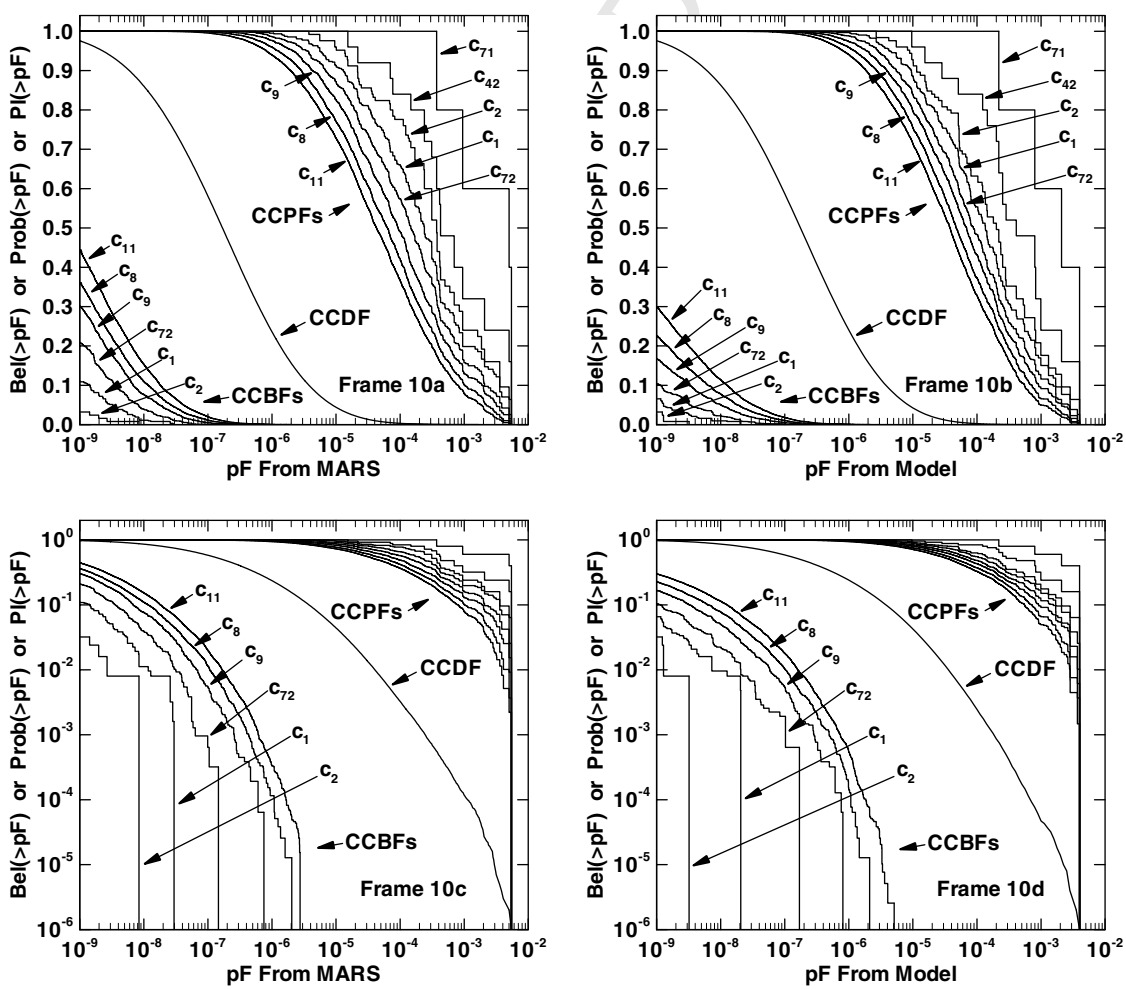

Fig. 10. Stepwise construction of CCBFs and CCPFs for pF with the evidence spaces for the individual components of **x** redefined to have 5 focal elements as indicated in conjunction with Fig. 8 and sequential inclusion of $c_{71}, c_{42}, c_2, c_{11}, c_{72}, c_9, c_8$ and c_{11}: (a) construction with MARS response surface approximation to log(pF) (left frames), and (b, d) construction with predicated values for log(pF) (right frames).

mental R^2 value of 0.06 in the MARS response surface construction would suggest (Table 5). Thus, there is not always an exact correspondence between incremental R^2 values and shifts in the locations of CCPFs. For perspective, Fig. 10 shows the results of a sequential construction of CCBFs and CCPFs in which c_{42} is the second rather than the sixth variable included the construction process. With this change in the order of variable consideration, the CCPFs now show a pattern of decreasing separation as more variables are incorporated into the CCPFs.

The sequential construction of CCBFs and CCPFs can be viewed a form of sensitivity analysis within the context of an evidence theory representation of uncertainty. Specifically, variable importance is indicated by the extent that the CCBFs and CCPFs change when a variable is entered into the construction process with its full evidence theory representation.

6. Discussion

Evidence theory is a promising alternative to probability theory for the representation of epistemic uncertainty when limited information is available. With evidence theory, a less structured representation of uncertainty is possible than is the case with probability theory.

Evidence theory representations of uncertainty can be interpreted in two different ways. With one interpretation, an evidence theory representation of uncertainty can be viewed as the specification of an incompletely defined probability space. With this interpretation, the belief associated with a set is the smallest probability that must be assigned to that set to complete the definition of the probability space, and the plausibility associated with a set is the largest probability that could be assigned to that set in a completion of the definition of the probability space. With the other interpretation, evidence theory provides a structure for reasoning under uncertainty. With this interpretation, the belief associated with a set is a measure of the amount of information that supports the truth of an assertion corresponding to the set, and the plausibility associated with a set is a measure of the lack of information that contradicts an assertion corresponding to the set.

Regardless of the interpretation, the mathematics of an evidence theory representation of uncertainty is the same. A particular challenge in this mathematics is the propagation of an evidence theory structure through a function which is computationally expensive to evaluate.

This presentation has described a sampling-based computational procedure for the propagation of an evidence theory representation of uncertainty through a computationally expensive function (i.e., a numerically demanding computer program). At the core of this procedure is the use of Latin hypercube sampling and nonparametric regression models to develop response surface approximations to analysis results of interest. This procedure provides a means to propagate an evidence theory representation of uncertainty through a function where more naïve sampling-based approaches will fail due to the high cardinality of the evidence space. Further, the stepwise nature of the propagation process provides sensitivity analysis results that can be interpreted in the context of evidence theory.

Acknowledgements

Work performed at Sandia National Laboratories (SNL), which is a multiprogram laboratory operated by Sandia Corporation, a Lockheed Martin Company, for the US Department of Energy's National Nuclear Security Administration under Contract No. DE-AC04-04AL85000. Review at SNL provided by L. Swiler and C. Sallaberry. Editorial support provided by F. Puffer, J. Ripple, and K. Best of Tech Reps, a division of Ktech Corporation.

References

[1] M.A. Christie, J. Glimm, J.W. Grove, D.M. Higdon, D.H. Sharp, M.M. Wood-Schultz, Error Analysis and Simulations of Complex Phenomena, Los Alamos Science 29 (2005) 6–25.
[2] I. Babuska, J.T. Oden, Verification and validation in computational engineering and science: basic concepts, Comput. Methods Appl. Mech. Engrg. 193 (36–38) (2004) 4057–4066.
[3] J.C. Helton, Uncertainty and sensitivity analysis in the presence of stochastic and subjective uncertainty, J. Stat. Comput. Simulat. 57 (1–4) (1997) 3–76.
[4] M.E. Paté-Cornell, Uncertainties in risk analysis: six levels of treatment, Reliab. Engrg. Syst. Safety 54 (2–3) (1996) 95–111.
[5] R.J. Breeding, J.C. Helton, E.D. Gorham, F.T. Harper, Summary description of the methods used in the probabilistic risk assessments for NUREG-1150, Nucl. Engrg. Des. 135 (1) (1992) 1–27.
[6] G. Apostolakis, The concept of probability in safety assessments of technological systems, Science 250 (4986) (1990) 1359–1364.
[7] J.C. Helton, J.D. Johnson, W.L. Oberkampf, An exploration of alternative approaches to the representation of uncertainty in model predictions, Reliab. Engrg. Syst. Safety 85 (1-3) (2004) 39–71.
[8] J.C. Helton, J.D. Johnson, C.J. Sallaberry, C.B. Storlie, Survey of sampling-based methods for uncertainty and sensitivity analysis, Reliab. Engrg. Syst. Safety 91 (10–11) (2006) 1175–1209.
[9] M.D. McKay, R.J. Beckman, W.J. Conover, A comparison of three methods for selecting values of input variables in the analysis of output from a computer code, Technometrics 21 (2) (1979) 239–245.
[10] J.C. Helton, F.J. Davis, Latin hypercube sampling and the propagation of uncertainty in analyses of complex systems, Reliab. Engrg. Syst. Safety 81 (1) (2003) 23–69.
[11] D. Dubois, H. Prade, Fuzzy Sets, Probability and measurement, Eur. J. Operat. Res. 40 (1989) 135–154.
[12] J.S. Wu, G.E. Apostolakis, D. Okrent, Uncertainty in system analysis: probabilistic versus nonprobabilistic theories, Reliab. Engrg. Syst. Safety 30 (1990) 163–181.
[13] P. Smets, Probability, Possibility, Belief: Which and Where? in: D.M. Grabbay, P. Smets (Eds.), Handbook of Defeasible Reasoning and Uncertainty Management Systems, Kluwer Academic Publishers, Boston, MA, 1998, pp. 1–24.
[14] D. Dubois, H.T. Nguyen, H. Prade, Possibility theory, probability theory and fuzzy sets: misunderstandings, bridges and gaps, in: D.M. Grabbay, P. Smets (Eds.), Fundamentals of Fuzzy Sets, Kluwer Academic Publishers, Boston, MA, 2000, pp. 343–438.
[15] G.J. Klir, Measures of uncertainty and information, in: D. Dubois, H. Prade (Eds.), Fundamentals of Fuzzy Sets, Kluwer Academic Publishers, Boston, MA, 2000.

UNCORRECTED PROOF

[16] T.J. Ross, J.M. Booker, W.J. Parkinson (Eds.), Fuzzy logic and probability applications: bridging the gap, Society for Industrial and Applied Mathematics, Philadelphia, PA, 2002.
[17] G.J. Klir, Generalized information theory: aims, results, and open problems, Reliab. Engrg. Syst. Safety 85 (1-3) (2004) 21–38.
[18] G.J. Klir, Uncertainty and Information: Foundations of Generalized Information Theory, Wiley, Hoboken, NJ, 2005.
[19] A.P. Dempster, Upper and lower probabilities induced by a multivalued mapping, Ann. Math. Stat. 38 (1967) 325–339.
[20] A.P. Dempster, Upper and lower probability inferences based on a sample from a finite univariate population, Biometrika 54 (2–3) (1967) 515–528.
[21] A.P. Dempster, A generalization of Bayesian inference, J Royal Stat. Soc., Ser. B 30 (1968) 205–247.
[22] G. Shafer, A Mathematical Theory of Evidence, Princeton University Press, Princeton, NJ, 1976.
[23] S. Ferson, R.B. Nelson, J. Hajagos, D.J. Berleant, J. Zhang, W.I. Tucker, L.R. Ginzburg, W.L. Oberkampf, Dependence in Probabilistic Modeling, Dempster–Shafer Theory, and Probability Bounds Analysis, SAND2004-3072, Sandia National Laboratories, Albuquerque, NM, 2004.
[24] C. Joslyn, J.C. Helton, Bounds on belief and plausibility of functionality propagated random sets, in: J. Keller, O. Nasraoui (Ed.), 2002 Annual Meetings of the North American Fuzzy Information Processing Society, Proceedings, 27–29 June 2002, IEEE, New Orleans, LA: Piscataway, NJ, 2002, pp. 412–417.
[25] C. Joslyn, V. Kreinovich, Convergence properties of an interval probabilistic approach to system reliability estimation, Int. J. General Syst. 34 (4) (2005) 465–482.
[26] C.B. Storlie, J.C. Helton, Multiple Predictor Smoothing Methods for Sensitivity Analysis, SAND2006-4693. Albuquerque, Sandia National Laboratories, NM, 2006.
[27] C.B. Storlie, J.C. Helton, Multiple predictor smoothing methods for sensitivity analysis: description of techniques, Reliability Engrg. System Safety, in press.
[28] C.B. Storlie, J.C. Helton, Multiple predictor smoothing methods for sensitivity analysis: example results, Reliability Engrg. System Safety, in press.
[29] J.C. Helton, J.D. Johnson, W.L. Oberkampf, C.J. Sallaberry, Sensitivity analysis in conjunction with evidence theory representations of epistemic uncertainty, Reliab. Engrg. Syst. Safety 91 (10-11) (2006) 1414–1434.
[30] D.W. Plummer, W.H. Greenwood, The history of nuclear weapon safety devices, Paper no. AIAA-1998-3464. AIAA/ASME/SAE/ASEE 34th Joint Propulsion Conference and Exhibit, Cleveland, OH, July 13–15, American Institute of Aeronautics and Astronautics, Reston, VA, 1998.
[31] J.C. Helton, J.D. Johnson, W.L. Oberkampf, Probability of loss of assured safety in temperature dependent systems with multiple weak and strong links, Reliab. Engrg. Syst. Safety 91 (3) (2006) 320–348.
[32] R.L. Iman, W.J. Conover, A distribution-free approach to inducing rank correlation among input variables, Commun. Stat.: Simulat. Comput. B11 (3) (1982) 311–334.
[33] J.C. Helton, F.J. Davis, Sampling-based methods, in: A. Saltelli, K. Chan, E.M. Scott (Eds.), Sensitivity Analysis, Wiley, New York, NY, 2000, pp. 101–153.
[34] J.H. Friedman, Multivariate adaptive regression splines (with discussion), Ann. Stat. 19 (1) (1991) 1–141.
[35] T.J. Hastie, R.J. Tibshirani, Generalized additive models, Chapman & Hall, London, 1990.
[36] D. Ruppert, M.P. Ward, R.J. Carroll, Semiparametric Regression, Cambridge University Press, Cambridge, 2003.
[37] J.S. Simonoff, Smoothing Methods in Statistics, Springer-Verlag, New York, NY, 1996.
[38] L. Breiman, J.H. Friedman, R.A. Olshen, C.J. Stone, Classification and Regression Trees, Wadsworth International, Belmont, CA, 1984.
[39] A.W. Bowman, A. Azzalini, Applied Smoothing Techniques for Data Analysis, Clarendon, Oxford, 1997.
[40] W. Härdle, Applied Nonparametric Regression, Cambridge University Press, Cambridge, 1990.

UNCORRECTED PROOF

Please cite this article in press as: J.C. Helton et al., A sampling-based computational strategy for the representation ..., Comput. Methods Appl. Mech. Engrg. (2007), doi:10.1016/j.cma.2006.10.049